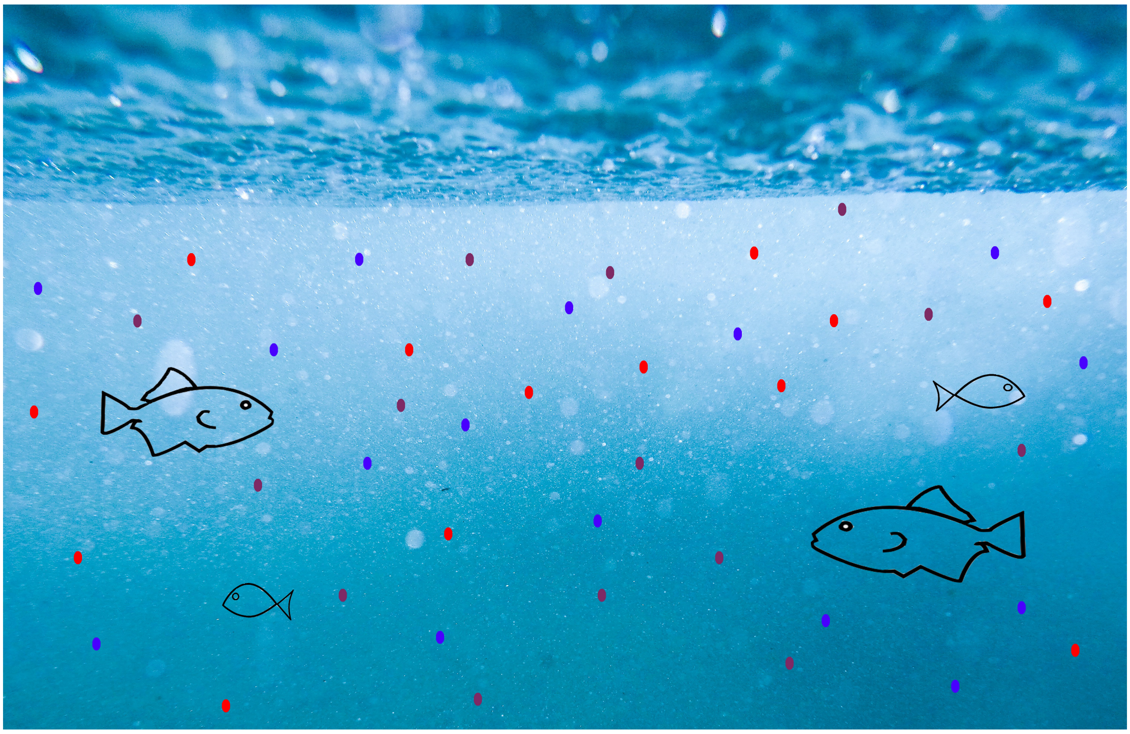

Particle Tracking of Microplastics in Aquatic Environments

Master's thesis in Applied Mechanics

SOURAV NANDAKUMAR

DEPARTMENT OF MECHANICS AND MARITIME SCIENCES

CHALMERS UNIVERSITY OF TECHNOLOGY
Gothenburg, Sweden 2021
www.chalmers.se

Master's thesis 2021:17

Particle Tracking of Microplastics in Aquatic Environments

Numerical method to track the trajectory of different Microplastics in water bodies

SOURAV NANDAKUMAR

Department of Mechanics and Maritime Sciences
Division of Fluid Dynamics
Chalmers University of Technology
Gothenburg, Sweden 2021

Particle Tracking of Microplastics in Aquatic Environments
Numerical method to track the trajectory of different Microplastics in water bodies
SOURAV NANDAKUMAR

Examiner: Gaetano Sardina, Department of Mechanics and Maritime Sciences

Master's Thesis 2021:17
Department of Mechanics and Maritime Sciences
Division of Fluid Dynamics
Chalmers University of Technology
SE-412 96 Gothenburg
Telephone +46 31 772 1000

Cover: Microplastic distribution in aquatic environment

Typeset in LaTeX
Printed by Chalmers Reproservice
Gothenburg, Sweden 2021

Particle Tracking of Microplastics in Aquatic Environments
Numerical method to track the trajectory of different Microplastics in water bodies
SOURAV NANDAKUMAR
Department of Mechanics and Maritime Sciences
Division of Fluid Dynamics
Chalmers University of Technology

Abstract

Microplastics in aquatic environments emerged as a leading environmental problem in recent times. The identification, standardisation and removal of those is a serious concern. This study aims at discussing the effect of biofouling on the vertical transport of plastic particles in laminar and turbulent flow conditions. The effects of turbulence are studied with a stochastic approach. All the studies are based on the Lagrangian Particle Tracking approach to track the trajectory of particles due to vertical transport accounting the seawater parameters of North Pacific. The effect of biofouling and the defouling is studied on both buoyant and non-buoyant particles.

In the turbulent flow condition, regardless of the type of plastic, for smaller radii all plastics behaved similar as the statistics shows that the turbulent fluctuations are dominant and the sediment velocity of the particle is negligible, thus meaning the particles behaves more as tracers

Keywords: Biofouling, Stochastic Tracking, Trajectory, Vertical Transport, Turbulent Dispersion.

Acknowledgements

I would like to express my heartfelt and profound gratitude to my supervisor Gaetano Sardina for his diligent supervision, inspiring guidance and encouragement throughout the course of my work. His ideas and constructive criticism have inspired me to work harder and complete this project successfully. His feedback and friendly attitude provided me with enough positive energy and also helped me to learn many concepts. Even in this pandemic time, the effective and frequent zoom meetings and umpteen number of conversations through emails are truly appreciable. I would also like to express my deepest gratitude to Jean Paul Mollicone for his unwavering support, collegiality and mentorship throughout this project. My special mention to Ananda Subramani Kannan for his support and feedback during the report writing process

I would also like to thank Florian Bourdrel, the author of the matlab code in which I adapted to use in this study. Without those, the studies could not have been started smoothly. Above all, I want to express my gratitude to my friends and family for constantly supporting me and pampering me with positive vibes even in this COVID pandemic situation.

Sourav Nandakumar, Gothenburg, May 2021

NOMENCLATURE

Abbrevations

LPT	Lagrangian Particle Tracking	
DNS	Direct Numerical Simulations	
DRW	Discrete Random Walk	
CRW	Continuous Random Walk	
CFD	Computational Fluid Dynamics	
PP	Polypropylene	
$LDPE$	Low density Polyethylene	
PS	Polystyrene	
PVC	Polyvinyl chloride	

Latin Symbols

z	Depth of ocean	m
t	Computational days	
V_s	Settling Velocity	ms^{-1}
A	Number of algae cells attached	
A_A	Ambient algae concentration	m^{-3}
D_*	Dimensionless particle diameter	
S_z	Salinity of seawater	$\mathrm{g.kg}^{-1}$
T	Temperature to sustain algae growth	^0C
I	Light intensity for algae growth	$\mu Em^{-2}s^{-1}$
m_A	Constant mortality rate	
Q_{10}	Temperature coefficient of respiration	
R_{20}	Constant respiration rate	
D_{pl}	Diffusivity of plastic particle	m^2s^{-1}
D_A	Diffusivity of algae cells	m^2s^{-1}
g	Acceleration due to gravity	ms^{-2}
$Chl-a$	Chlorophyll a concentration	$(\mathrm{mg.C})^{-1}$
u_f	Fluid velocity	ms^{-1}
w_{sink}	Settling velocity	ms^{-1}
τ_f	Stress tensor	
C_D	Coefficient of Drag	
Re	Reynolds Number	
Re_λ	Reynolds Number based on Taylor scale	
Ra	Rayleigh Number	
Pr	Prandtl Number	
r_{pl}	Plastic initial radius	m
r_{tot}	Plastic total radius	m

t_{bf}	Biofilm thickness	m
V_{pl}	Plastic volume	m^3
V_{bf}	Biofilm volume	m^3
V_{tot}	Total volume	m^3
Greek Symbols		
μ_A	Growth rate of algae	s^{-1}
β_A	Encounter kernel rate	$m^3 s^{-1}$
α_f	Void fraction of continuous phase	
ρ_f	Density of continuous phase	kg m^{-3}
ζ	Random number with normal distribution	
σ	RMS value of velocity	ms^{-1}
ω_*	Dimensionless sinking velocity	
θ_{pl}	surface area of the plastic particle	m^2
$\mu_{sw,z}$	Dynamic sea water viscosity	kg $m^{-1} s^{-1}$
$\nu_{sw,z}$	Kinematic sea water viscosity	$m^2 s^{-1}$
ρ_{tot}	Total density of particle	kg m^{-3}
$\rho_{sw,z}$	Sea water density	kg m^{-3}
ρ_{pl}	Particle density	kg m^{-3}
ρ_{bf}	Biofilm density	kg m^{-3}

Contents

List of Figures

List of Tables

1

Introduction

1.1 Background

In 1907, a revolutionary invention took place in the world. It was none another than 'Fully synthetic plastics'[1] (referred to invention of Bakelite). After the invention of fully synthetic plastics, we have seen a tremendous advancement in the field over these years. It is very interesting and at the same time horrifying to see the growth of plastics and the everyday use. We are facing many environmental hazards with the non degradable object that can eventually harm us if not treated in a proper way, on an environment point of view.

As we all are aware, plastics are one of the main components contributing to pollution throughout the environment and have been found in seawater, freshwater, food and drinking water. It was estimated that the worldwide load of plastic on the open ocean surface was far less than expected. This is due to the fragmentation of plastics into microscopic fragments. They are accumulated in the pelagic zone and sedimentary habitats[28]. It is generally because of the sinking of certain fragments into the ocean depth [2]. It is expected that by 2050, there will be more plastic in the ocean than fish, if not properly handled. Plastic debris are present in plethora of shapes and sizes. Those plastic debris which is less than 5 mm in size are termed as "microplastics".

Microplastics originate from many sources, including the very tiny polyethylene particles used as exfoliants to health and beauty products and by fragmentation of larger plastic debris[3, 4]. They are also formed due to the degradation of those plastics found in beaches or water[7]. The degradation process depends on factors such as UV radiation, salinity, temperature etc and the degradation process can take very long time.[7, 8]. It can pass through the available water filtration systems that we have today and has the ability to reach organisms in our water bodies causing high threat to aquatic life. One major problem is that the aquatic life will mistake microplastics as food and consume it, which causes serious health issues.

Recent studies suggest that microorganisms such as algae, bacteria, protozoans and fungi are formed on these microplastics inside water bodies [5] is affecting buoyancy of the plastic. The accumulation of those microorganism on the plastic increases the plastic density . When the particle density is increased more than the seawater density, these particles start to settle. The phenomenon discussed is referred as 'biofouling', and in this Thesis work, a biofouling model developed by Kooi et al.[6] is used. The vertical motion stops once the density of the particle equals the seawater density. Due to several factors like lack of sunlight, grazing or dissolution of carbonates in acid water, another phenomenon called defouling occurs. The density of the particle is decreased and the plastic debris is transported back upwards.

1.2 Motivation

The social need of lowering the impact caused by plastic pollution is a global concern. Especially when the microplastics pollution is taken into account, they floats in the water bodies as well as in the air we breathe (since they are lightweight). It is now widely discussed over the globe. Tracking the microplastics debris can contribute to the aquatic life by finding solutions to eradicate it.

The motivation to contribute to issues linked with microplastics debris paved the way for the selection of this Thesis topic. It can lead to further researches so that the debris can be efficiently located making the removal easier. Microplastics are consumed by every form of living beings living in oceans or other water bodies. But it is indirectly consumed by the predators of aquatic organisms including human beings. In this process, no living species is kept apart as it includes most kind of species. Not only the current generation of living beings are affected, but their coming generations and those animals which consume them too[11] because they plastics are non biodegradable.

The fate of microplastics in the environment should be determined by predicting its source and trajectory . It is necessary to map the microplastic distribution across the world. For this to be effective, the identification and standardisation of microplastics needs to be done[9]. This thesis work can contribute to a more sustainable environment and increases the life expectancy of aquatic animals by which indirectly it contributes to human mankind since humans are predators of those aquatic animals. As responsible living beings of mother earth, it is each individuals duty to support for the relief of this global crisis. The strongest motivation for the project is to be able to predict their trajectory as it can be useful to identify zones of preferential accumulation of the microplastics.

1.3 Vertical motions of microplastics due to biofouling

Buoyant plastics are those with lower density than the seawater whereas non-Buoyant plastics are vice-versa. The density variation aims to the fact that the buoyant plastics should float on the surface while the later sinks. But, as previously mentioned the initially buoyant microplastics will sink after a certain time. This is explained with the biofouling model developed by Kooi et al. [6].

As discussed earlier, for the microplastics that are floating in the ocean surface, after a certain time there is attachment or accumulation of certain organisms. When they

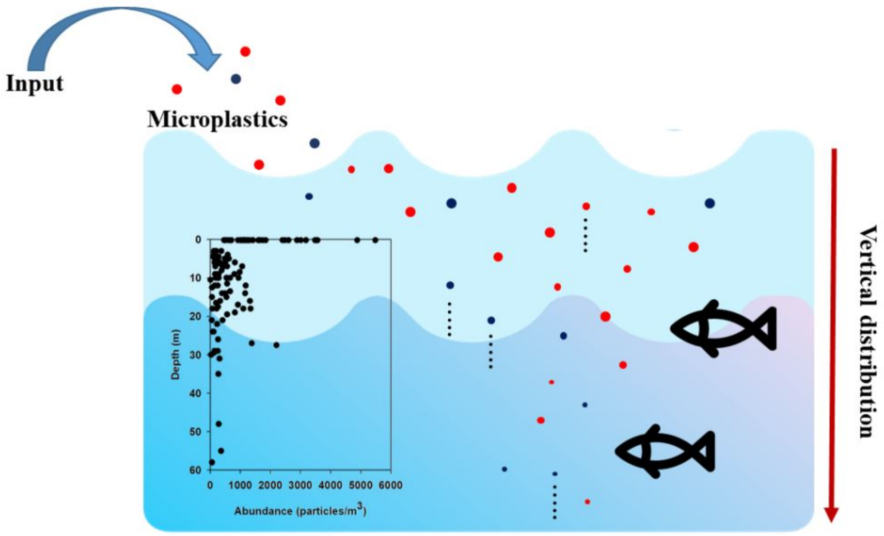

Figure 1.1: Vertical distribution of Microplastics[19]

floats on the surface of water bodies, it readily develops extensive surface fouling which instantly covers the surface with a biofilm followed by an algal mat and then a colony of invertebrates[10]. This leads to the increase in density which once crosses the seawater density accounts for the sinking of the buoyant plastic. Once defouling starts (because of the factors introduced in Section 1.1) the microplastics are carried back to ocean surface and thereby it oscillates due to continuous switching of biofouling and defouling. The vertical motions of the microplastics are explained with the above process and the vertical distribution of plastics in oceans is as shown in figure 1.1.

1.4 Objectives and Methodology

The primary goal of the project is to track the microplastics position inside oceans and to calculate the time required for the debris to oscillate in the domain. Tracking the trajectory of microplastics will play a crucial role in the future of a sustainable environment. Determining the position of these microplastics can map them which helps in identifying the zones of preferential accumulation of the microplastics in oceans.

The tracking will be done for different flow cases like, in quiescent flow condition, a turbulent flow condition and both type of flows with and without stratification. To solve the equations and to track the debris, a Matlab code is used which is an adaptation of work done by Florian Bourdrel [12]. The code includes all the relevant parameters used to track the particle. It includes the determination of sinking velocity, calculation of biofilm thickness, the number of attached algae to the surface of plastic and also the Lagrangian particle tracking scheme which determined the microplastic position.

The code from Bourdrel was further developed to find the sinking velocity with correction for stratification. Another main change was the replacement of Matlab inbuilt ode23 solver with the third-order low-storage Runge-Kutta scheme. For implementation of Turbulence flow, the kinetic energy and dissipation values from studies of Stephan Juricke et al.[13] and Walter et al.[14] respectively are used. The turbulent velocity is determined using Langevin equation [15, 16] with a Continuous Random Walk Model which is Monte Carlo method. It solves the numerical problem with a random sampling, which is a stochastic term in the Langevin equation consisting of random numbers which mimics turbulent diffusion. Then for both laminar and turbulent flow cases, the particle position and the number of attached algaes along with the time is calculated with appropriate time step for different variety of microplastics(varying density and radius). In this study mainly two buoyant and two non-buoyant plastics namely Polypropylene(PP), Low-density polyethylene(LDPE) and Polystyrene(PS), Polyvinyl chloride(PVC) respectively are used (Density = 840, 920, 1050 & 1380 $kg.m^{-3}$).

The updated findings can be incorporated into an in house code to perform CFD analysis in future. This will contribute to future researchers to provide more input to the research area of 'Microplastics inside oceans' and also in a lesser time than usual. This also paves a way to explore much more phenomenons in this topic.

2

Theory

The current project work mainly focus on individual tracking of microplastics and hence as a result Lagrangian Particle Tracking method is used. The plastic particle is considered as a single particle and is implemented using the Matlab code which is modified from Bourdrel[12].

In the theory chapter, the particle motion, the Lagrangian particle tracking, the turbulence model using Monte Carlo method and the numerical schemes used to solve the equations are discussed in detail.

2.1 Particle Motion

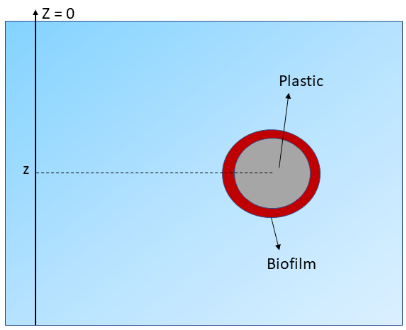

Figure 2.1: Microplastic affected by biofouling in water

The main assumption for the whole study is that the given microplastic or particle is spherical in shape. Addition to it, the attached biofilm is also considered spherical. The main purpose of the assumption is to simplify the calculations. The depth at which the particle is reached is measured from center of the particle as shown in figure 2.1.

The continuous phase is modelled with the help of profiles of temperature,salinity,density and chlorophyll as used by Kooi et al.[6] and Bourdrel[12].Since the biofouling phenomenon is also taken into consideration along with particle settling velocity, the attached algae growth is also used.

$$\frac{dz}{dt} = V_s(z,t) \tag{2.1}$$

where V_s is the settling velocity of the particle and z,t are the depth and time respectively.

$$\frac{dA}{dt} = \frac{\beta_A A_A}{\theta_{pl}} + \mu_A(T,I)A - m_A A - Q_{10}^{(T-20)/10} R_{20} A \tag{2.2}$$

where L.H.S is the attached algae growth and for R.H.S,

The I term accounts for the collision of plastic particle with algae while fouling[20] and the II term measures the algal growth with respect to temperature and light[21]. The term $m_A A$ quantifies mortality[21] while the last term of R.H.S model the respiration[22].

In equation 2.1, the settling velocity is given by,

$$V_s(z,t) = -\left(\frac{\rho_{tot} - \rho_{sw,z}}{\rho_{sw,z}} g\omega_* \nu_{sw,z}\right)^{1/3} \tag{2.3}$$

where ω_* is the dimensionless sinking velocity with ρ_{tot} and $\rho_{sw,z}$ are the total density of the plastic (combined with the attached algae) and density of seawater at specified depth z .Also $\nu_{sw,z}$ is the kinematic viscosity of the seawater and by default g is the acceleration due to gravity. ω_* is calculated from another dimensionless particle diameter D_* as

$$\omega_* = 1.74 * 10^{-4} D_*^2 \qquad for \quad D_* < 0.05 \tag{2.4}$$

$$\begin{aligned} log(\omega_*) = &-3.76715 + 1.92944 logD_* - 0.09815(logD_*)^2 \\ &- 0.00575(logD_*)^3 + 0.00056(logD_*)^4 \\ &for \quad 0.05 \geq D_* \geq 5x10^9 \end{aligned}$$

where,

$$D_* = \frac{(\rho_{tot} - \rho_{sw,z}) g D_n^3}{\rho_{sw,z} \nu_{sw,z}^2} \tag{2.5}$$

where D_n is the equivalent spherical diameter[23, 24].

Due to the homogeneity of the algal distribution which contributes the biofilm and the spherically assumed particles the total density of the particle is,

$$\rho_{tot}(z,t) = \frac{r_{pl}^3 \rho_{pl} + [(r_{pl} + t_{bf})^3 - r_{pl}^3]\rho_{bf}}{(r_{pl} + t_{bf})^3} \tag{2.6}$$

where the terms in the R.H.S are radius of plastic (r_{pl} in m), biofilm thickness (t_{bf} in m), density of plastic (ρ_{pl} in kg/m^3) and the density of the biofilm(ρ_{bf} in kg/m^3). These terms are calculated as

$$t_{bf} = (V_{tot}\frac{3}{4\pi})^{1/3} - r_{pl} \tag{2.7}$$

$$V_{tot} = V_{bf} + V_{pl} \tag{2.8}$$

$$V_{pl} = \frac{4}{3}\pi r_{pl}^3 \tag{2.9}$$

$$\theta_{pl} = 4\pi r_{pl}^2 \tag{2.10}$$

$$V_{bf} = (V_A A)\theta_{pl} \tag{2.11}$$

Here θ_{pl} is the particle surface area in m^2 while V_{tot}, V_{bf}, V_{pl} and V_A are the total volume, biofilm volume, the plastic volume and the volume of algae cells respectively in m^3 and A is the number of algae cells attached.

In equation 2.3, the kinematic viscosity of seawater is calculated as,

$$\nu_{sw} = \frac{\mu_{sw,z}}{\rho_{sw,z}} \tag{2.12}$$

where the sea water dynamic viscosity is calculated as,

$$\mu_{sw,z} = \mu_{w,z}(1 + AS_z + BS_z^2) \tag{2.13}$$

in which water dynamic viscosity,

$$\mu_{w,z} = 4.284410^{-5} + \frac{1}{0.156(T_z + 64.993)^2 - 91.296} \tag{2.14}$$

and the constants A,B are

$$A = 1.541 + 1.998 * 10^{-2}T_z - 9.52 * 10^{-5}T_z^2 \tag{2.15}$$

$$B = 7.974 - 7.561 * 10^{-2}T_z + 4.724 * 10^{-4}T_z^2 \tag{2.16}$$

Also, the temperature, salinity and seawater density is determined as a function of depth to keep a profile study using the following equations,

$$T_z = T_{surf} + (T_{bot} - T_{surf})\frac{z^P}{z^P + z_c^P} \tag{2.17}$$

$$S_z = c_1z^5 + c_2z^4 + c_3z^3 + c_4z^2 + c_5z + c_6 \qquad for \;\; z > z_{fix} \tag{2.18}$$

$$\rho_{sw,z} = a1+a2T_z+a3T_z^2+a4T_z^3+a5T_z^4+b1S_z+b2S_zT_z+b3S_zT_z^2+b4S_zT_z^3+b5S_z^2T_z^2 \tag{2.19}$$

In the salinity profile, if the condition in equation 2.18 is not met, then a constant value of salinity is assumed for those depths which do not meet the criteria. Also the values of the constants a_n, b_n & c_m is given in Appendix A.1 with $n = 1, 2, 3, 4, 5$ and $m = 1, 2, 3, 4, 5, 6$

Now when we take the case of equation 2.2, in the first term, β_A is the encounter kernel rate which consists of different type of collisions such as Brownian motion, settling of the plastic and the advective shear of algae. A_A is the ambient algae concentration which depends on chlorophyll-a local concentration[25].

$$\beta_{A_{brownian}} = 4\pi(D_{pl} + D_A)(r_{tot} + r_A) \tag{2.20}$$

$$\beta_{A_{settling}} = \frac{1}{2}\pi r_{tot}^2 |V_s| \tag{2.21}$$

$$\beta_{A_{shear}} = \frac{4}{3}\gamma(r_{tot} + r_A)^3 \tag{2.22}$$

where, Diffusivity of the plastic particle is

$$D_{pl} = \frac{k(T + 273.16)}{6\pi\mu_{sw} r_{tot}}$$

and Diffusivity of the algae cells are

$$D_A = \frac{k(T + 273.16)}{6\pi\mu_{sw} r_A}$$

and for the cholorophyll-a concentration the follwing equation was used

$$Chl - a : C = 0.003 + 1.0154 e^{0.050T} e^{-0.0591 I_z/10^6} \mu' \tag{2.23}$$

and the vertical profile is modelled as a function of depth as[25, 26]

$$Chl(z) = \frac{Chl - a(z)}{Chl - a_{Z_{base}}} = C_b - sz + C_{max} e^{-((z-Z_{max})/\Delta z)^2} \tag{2.24}$$

When the second term in equation 2.2 is examined,

$$\mu(T_z, I_z) = \mu_{opt}(I_z)\Phi(T_z) \qquad for \quad T_{min} < T_z < T_{max} \tag{2.25}$$

where $\mu_{opt}(I_z)$ is the growth rate of algae under optimal conditions and $\Phi(T)$ is the growth rate influence under temperature[27] as,

$$\mu_{opt}(I_z) = \mu_{max} \frac{I_z}{I_z + \frac{\mu_{max}}{\alpha}\left(\frac{I_z}{I_{opt}} - 1\right)^2} \tag{2.26}$$

$$\Phi(T_z) = \frac{(T_z - T_{max})(T_z - T_{min})^2}{(T_{opt} - T_{min}) * ((T_{opt} * T_{min}(T_z - T_{opt}) - (T_{opt} - T_{max}(T_{opt} + T_{min} - 2T_z))} \tag{2.27}$$

with $I_z = I_0 e^{\epsilon z}$ and $I_0 = I_m sin(2\pi t)$ along with $\epsilon = \epsilon_w + \epsilon_p Chl - a$

Hence it is straightforward that the first two terms of equation 2.2 accounts for biofouling effects while the last two accounts for defouling effects. The mortality term is modelled using constant Mortality rate of 0.39 while in the last term, constant respiration rate of 0.1 and the temperature coefficient of respiration, $Q_{10} = 2$ is used.

With the equations 2.1 & 2.2, the vertical motion of the given microplastics are estimated and the Lagrangian particle tracking is used to track the trajectories of the microplastics as discussed in following section.

2.2 Lagrangian Particle Tracking

The dispersed phase as discussed is modelled using Lagrangian Particle tracking method. The general equation of motion of single particle corresponds to,

$$m_p \frac{dv_p}{dt} = F_{total} \tag{2.28}$$

where $F_{total} = F_D + F_B + F_G + F_A + F_H + F_L + F_{Brownian} + F_{other}$.

where the forces defined in the equations are drag force, buoyancy force, gravitational force, added mass force, history force, lift force, Brownian force and all other forces respectively. The other forces include Magnus Lift forces, Saffmann Lift forces, Pressure Gradient Force, Thermophoretic forces etc.

The trajectory of particle in this study is mainly influenced by the biofouling dynamics and hence the particle motion is governed as in Section 2.1 with coupled equations of particle trajectory and effect of biofouling. The third-order low-storage Runge-Kutta method which is an explicit method is used in this study to solve the equations to get the positions of the particle as already discussed.

2.3 Turbulence Modelling

The turbulent dispersion of particles due to the turbulence of carrier phase is modelled for turbulent flow cases. The turbulent time scale was also found which is necessary to incorporate the effect of turbulence. The instantaneous velocity is given by,

$$u = \overline{u} + u^{'} \tag{2.29}$$

where, $\overline{u}$ is the mean velocity and $u^{'}$ is the fluctuating velocity.The value of $\overline{u}$ can be found directly while $u^{'}$ needs to be modelled using stochastic equations. Basically there are two models which are extensively used to model homogeneous turbulence. They are as follows,

2.3.1 Discrete Random Walk Model

In Discrete Random Walk Model (DRW),the stochastic tracking and modelling of fluctuating component $u^{'}$ is done. It is assumed that the particle lies in the turbulent eddy and will stay until the eddy is dissipated. Once the eddy disappears, the particle then walks randomly or goes to another eddy. The lifetime of an eddy in terms of turbulent kinetic energy(k) and dissipation(ϵ) can be quantified as,

$$\tau_l = C_l \frac{k}{\epsilon} \tag{2.30}$$

The fluctuating component $u^{'}$ is modelled as,

$$u^{'} = \zeta \sqrt{\frac{2k}{3}} \tag{2.31}$$

where ζ is a random number with normal distribution. Isotropy is assumed for the fluctuating component and can be used to achieve statistically significant sampling with large number of tries.But in certain cases like wall bounded cases etc, isotropy cannot be assumed and is a concern. Thus DRW estimation is poor for even simple geometries because of strong over prediction of deposition.

2.3.2 Continuous Random Walk Model

In Continuous Random Walk Model(CRW), the stochastic tracking and particle dispersion modelling is much more physical. It is because the velocity of carrier phase influenced by particles continuously fluctuates with time. In order to model the stochastic part or the Brownian velocity fluctuations,original Langevin Equation is used.For implementing homogeneous turbulence, stochastic Langevin equation is in frame.The carrier phase velocity is same as in equation 2.29. Unlike the Discrete Random Walk Model, the fluctuations are more continuous in Continuous Random Walk Model. The Langevin equation is used to mimic turbulence so that the fluctuating velocity is modelled as ,

$$\frac{du_i^{'}}{dt} = -\frac{u_i(t)}{\tau_i} + \frac{2}{\sqrt{\tau_i}} \sigma_i \zeta_i(t) \tag{2.32}$$

where the index i can be x,y or z direction.τ_i is the Lagrangian time scale, $\sigma_i = \sqrt{\overline{u_i^{'2}}}$ is the root mean square value of the fluctuating velocity and $\zeta_i(t)$ corresponds to a random vector with Gaussian white noise process . The first term of the Langevin equation (equation 2.32) refers to the deterministic part (damping) while the last term is the stochastic part. The L.H,S of the equation 2.32 is the increment of the fluctuating velocity so that velocity is incremented in each time step.In this study direct Monte Carlo method is used with a modified Langevin Equation[16].

The Turbulent length scale in terms of kinetic energy and dissipation is quantified as,

$$\tau_i = \frac{4}{3C_0}\frac{k}{\epsilon} \tag{2.33}$$

where, the constant $C_0 = \frac{6.5}{(1+140Re_\lambda^{-4/3})^{3/4}}$ and the Reynolds number is based on Taylor scale and is defined as

$$Re_\lambda = \sqrt{\frac{20k^2}{3\nu\epsilon}}$$

2.4 Numerical Modelling

The Numerical modelling schemes are used to interpolate and discretize approximate solutions for ordinary differential equations. As discussed in section 1.4, Kooi et al. and Bourdrel[6, 12] used the inbuilt ode23 solver to solve the ordinary differential equation which is replaced as discussed before.

2.5 Stokes Drag

The drag force acting on spherical particles under low Reynolds Number or for creeping flow can be estimated with an expression using Stoke's Law.

$$F_D = 6\pi\mu r_p u \tag{2.34}$$

where r_p is the radius of the particle and u is the settling velocity.

For the flows which are having particle Reynolds number greater than unity,the estimated drag force is equated with the gravity force and the sedimentation velocity is extracted which is a nonlinear equation also termed as the Non Linear Stokes Drag,

$$C_D\frac{1}{2}\rho_f u^2\frac{\pi d^2}{4} = (\rho_p - \rho_f)g\frac{4\pi}{3}\left(\frac{d}{2}\right)^3 \tag{2.35}$$

where the expression of C_D will be,

$$C_D = \frac{24}{Re_p}(1 + 0.15 * Re_p^{0.687}) \tag{2.36}$$

with Re_p is the Reynolds number of the particle, ρ_f and ρ_p are the fluid and particle density respectively and g is the acceleration due to gravity.

3

Methods

The different methodology used for the completion of the study will be discussed in detail in this chapter.

3.1 Case Setup

The case setup is discussed more in detail. The plastic particle is having a radius of r_{pl} where the biofilm is having a thickness t_{bf}. So the total radius counts to $r_{tot} = r_{pl} + t_{bf}$. As discussed in Section 1.1, under certain conditions the plastic get attached with algaes and the configuration in figure 2.1 is made.

The simulation is done with respect to seawater parameters of North pacific Ocean. All the cases (different size and density) have initial condition, $t = 0$ with the plastic initially at surface (at $z = 0$) of the ocean without starting of the biofouling phenomena. So the particle is initially free from any algae attached ($A = 0$) to it.The ocean floor is set to be at $4000m$ depth.The geometry setup is as shown in figure 3.1

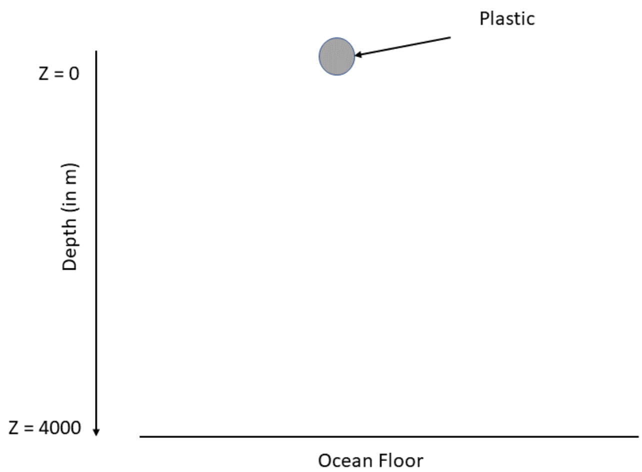

Figure 3.1: Geometry Setup

The plastics used for the study are as in table 3.1. The first two are the initially buoyant plastics while the last two are the non-buoyant plastics with their density accordingly. All the plastics are simulated for plastic radius of $r_{pl} = 1e-3$, $1e-4m$, $1e-5m$ & $1e-6m$.

Plastic	**Density** $(kg.m^{-3})$
$Polypropylene(PP)$	840
$LowDensityPolyethylene(LDPE)$	920
$Polystyrene(PS)$	1050
$Polyvinylchloride(PVC)$	1380

Table 3.1: The plastics used in this study along with their densities

3.2 Validation

Bourdrel [12] did the simulations for different amount of time for all the cases and each and every cases has been reproduced with the new solver. For introducing turbulence to the flow the Runge-Kutta scheme is used as it is more useful to incorporate the stochastic model compared to ode23 solver.

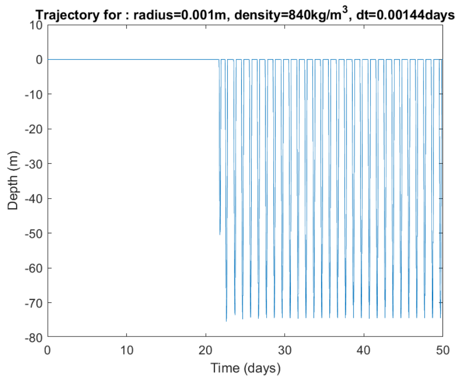

(a)

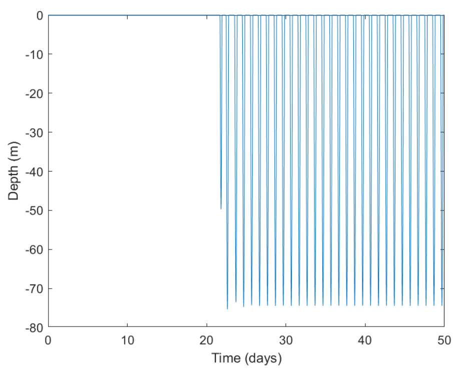

(b)

Figure 3.2: Position of initially buoyant microplastic, PP ($r = 1e{-}3m$) determined using (a) ODE23 solver (b) Runge-Kutta Scheme

Figure 3.2 and figure 3.3 ensures the validation of Runge-Kutta scheme against the ODE23 solver used in Matlab. In figure 3.2 the initially buoyant PP plastic with radius $1e-3m$ is simulated for 50 days using both the ODE23 and Runge-Kutta scheme. While in figure 3.3 , the non-buoyant PS plastic with radius $1e-3m$ is simulated for 10 days.Both the plots are tracking the trajectory of the given plastic until the input simulation days. It is very clear that the Runge-Kutta scheme is producing the same plots. Since the turbulent fluctuations are modelled and added in the particle trajectory equation, it is more easy in Runge-Kutta scheme. As a result, it has been used throughout the study.

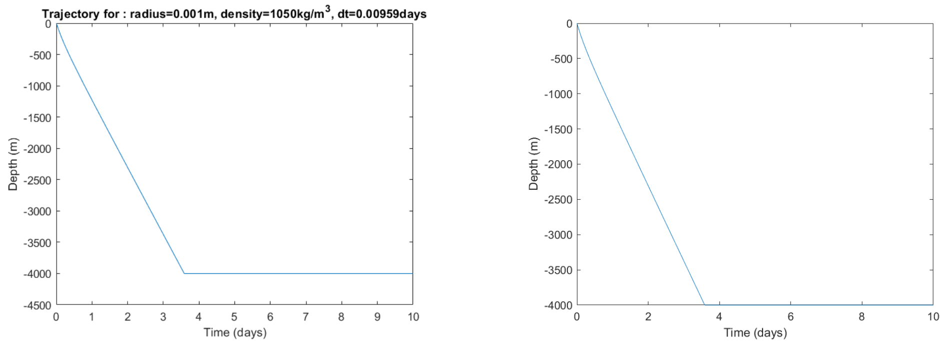

(a) (b)

Figure 3.3: Position of non-buoyant microplastic, PS ($r = 1e - 3m$) determined using (a) ODE23 solver (b) Runge Kutta Scheme

In figure 3.2, the horizontal line until approximately 21 days means that, the plastic is floating above the sea and once enough algae is attached to the particle, the plastic density is increased in which it becomes more than the sea water density which in turn cause the plastic to sink. The oscillations in the plot depicts the alternating biofouling and defouling phenomena as well. While in figure 3.3, since the plastic is non-buoyant, it starts to sediment as soon as the plastic is taken to the ocean top and once it reaches the ocean floor ($z = 4000m$), it stays there forever.

3.3 Stokes Drag

The theory behind Stoke's drag has been explained in section 2.5. Now, here it is implemented in Matlab replacing the original equation for determination of the Settling velocity in such a way that the drag is equated with the buoyancy analytically. The same method goes for both Linear and Non-Linear Stokes drag i.e, for the cases of $Re << 1$ and $Re >> 1$.

3.3.1 Linear Stokes Drag

As been discussed the Linear Stokes Drag equation is used for $Re << 1$ in which the coefficient of drag will be,

$$C_D = \frac{24}{Re_p} \tag{3.1}$$

The above equation is equated against buoyancy equation and the settling velocity is achieved as

$$w_{sink} = 9.81 * 4 * r_{pl}^2 * r_0^2 * \frac{\rho_{tot} - \rho_f}{\rho_f * 18 * \nu_0 * \nu} \tag{3.2}$$

where, w_{sink} is the settling velocity and ν_0 and r_0 is multiplied to non dimensionalize the equation.

The Linear Stokes Drag equation is used to find out the settling velocity of PP Plastic of radius $1e - 5m$ as in figure 3.4. It can be seen that the figures doesn't match since the Reynolds number of the flow is not always less than unity or in other words it is not creeping flow.Hence this method cannot be used further since we are accounting for flows with higher Reynolds number. Hence an adaptation is discussed in next subsection in which the coefficient of drag equation is slightly improved to account for higher Reynolds number.

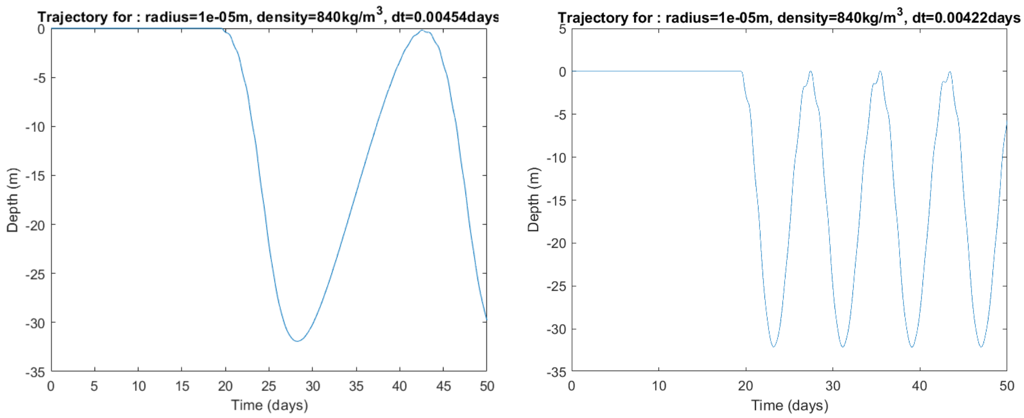

(a) (b)

Figure 3.4: Position of initially buoyant microplastic,PP ($r = 1e-5m$) determined using (a) Original code as in Bourdrel[12] (b) Linear Stokes Drag equation

3.3.2 Non-Linear Stokes Drag

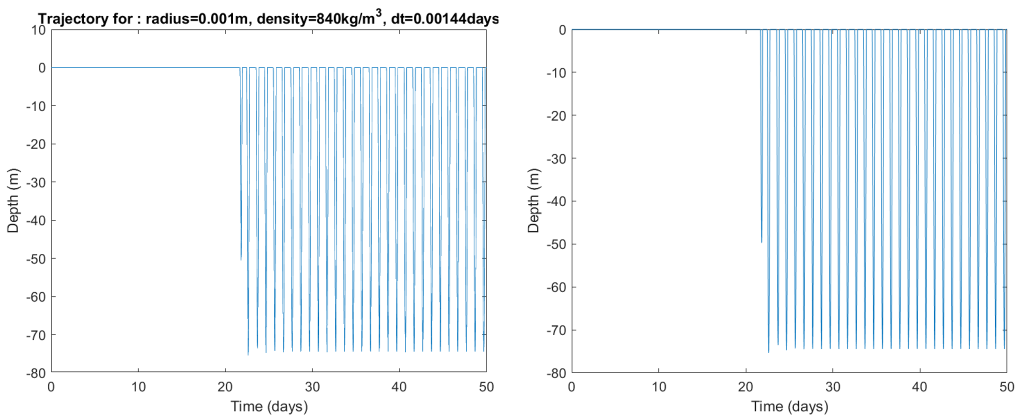

(a) (b)

Figure 3.5: Position of initially buoyant microplastic,PP ($r = 1e-3m$) determined using (a) Original code as in Bourdrel[12] (b) Non-Linear Stokes Drag equation

In figure 3.5, the comparison of particle position of PP microplastic with radius $1e-3m$ is shown. It is very clear that the results are matching with the method used in original code by Bourdrel [12]. The results were matching for other cases as well. This subsection deals with the implementation of Non-Linear stokes drag equation used to determine the sediment velocity of the plastic equating the buoyancy equation with the drag force equation when the Reynolds number is much greater than unity. The C_D for such cases are improvised using equation 2.36. The sinking velocity is found out from this equation and is coded in matlab as,

$$w_{sink} = \frac{\nu_0 \nu Re}{(2 r_{pl} r_0)} \tag{3.3}$$

where Re is obtained from taking the non-linear equation into account with Matlab using the roots of the non linear equation fzero function. The codes are given in the Appendix B.1.

3.4 Time Step

The time step used for the entire simulation is $1e-3$. The plots with different time steps for a PP plastic with radius $1e-3m$ is in figure 3.6. It can be inferred that $dt = 1e-3$ is the optimum time step from the plots.

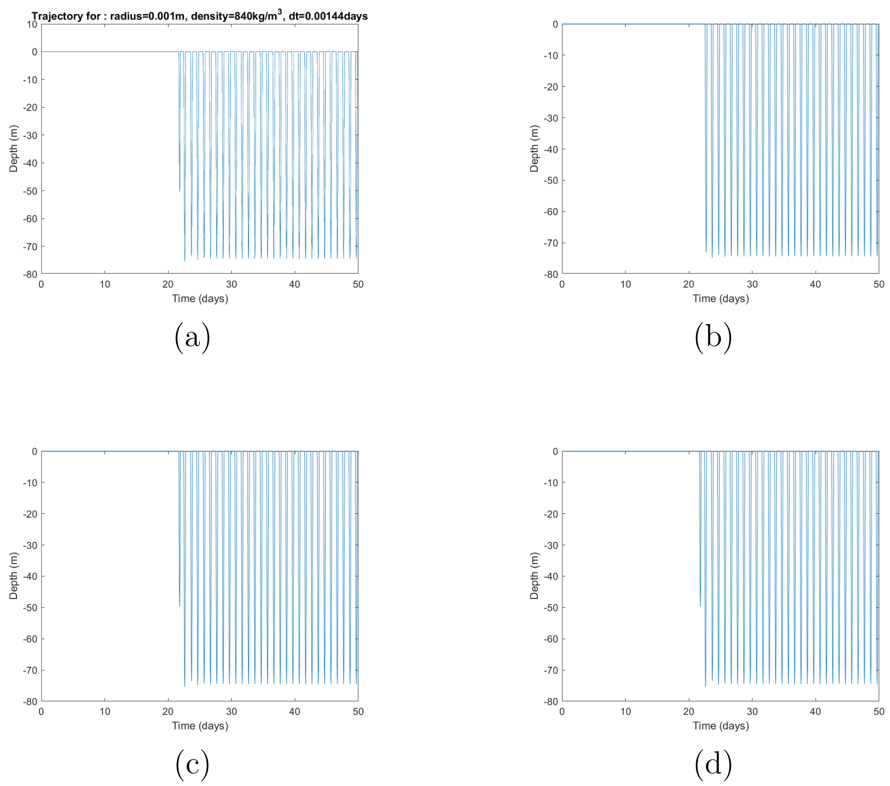

Figure 3.6: Position of initially buoyant microplastic,PP ($r = 1e-3m$) determined using (a) code as in BOURDEL[12] (b) $dt = 0.01$ (c) $dt = 0.001$ (d) $dt = 0.0001$

3.5 Turbulence Modelling

The turbulence dispersion of the carrier phase is explained in section 2.3 and 2.3.2. The fluctuating velocity of the carrier phase is found from the stochastic equation in which is the Langevin equation[15, 16]. The Langevin time scale and dissipation is taken from studies of Stephen Juricke et al.[13] and Walter et al.[14] and is as in figure 3.7. For the Turbulent Kinetic energy profile, after depth of 1400m, the value is assumed to be constant.

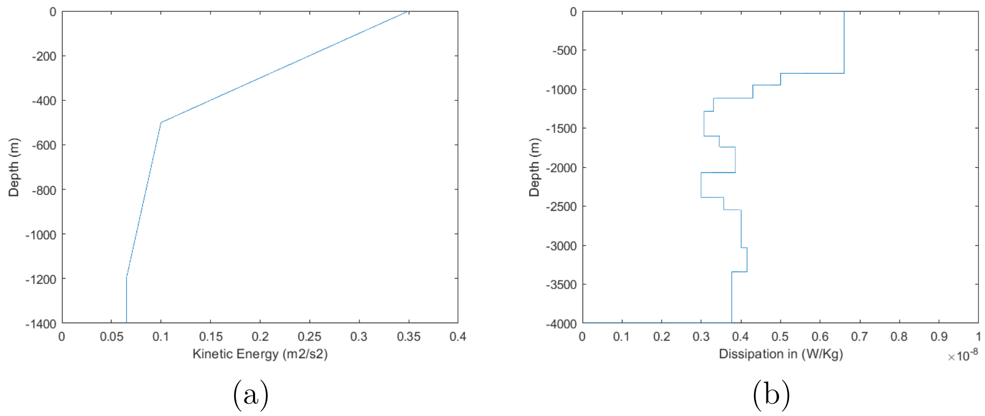

Figure 3.7: (a) Turbulent Kinetic energy profile[13] (b) Dissipation profile[14]

Once the values are obtained it is again fed into the Runge-Kutta scheme to obtain the fluctuating velocity. The discretization and implementation of these profiles in Matlab code is in the appendix inside the codes for the turbulent flow which is discussed in the Result Section.

4

Results

4.1 Laminar Flow Case

All the buoyant and non buoyant plastics are simulated in the laminar flow model. The validation and the previous case by BOURDREL[12] also did the same. So in order to know the average position and time fraction of each plastics, these are ran for more number of computational days. By this way the convergence was also checked as the recurring and stable values of the average position of the plastic confirmed the simulation has converged. The time fraction is a measure to find the fraction time in which the plastic was under the ocean top. In other words, the fraction time when the plastic is below the depth of $z = 0m$. For accuracy, in this study instead of $z = 0m$, $z = 1m$ is considered. Along with the particle trajectory, average position and time fraction, other plots such as biofilm thickness, number of attached algaes, plastic total density and the velocity is plotted.

4.1.1 PP Plastic

4.1.1.1 Particle Position

The particle position for PP plastic when the simulations were run for 500 days is as in figure 4.1. Four different sizes of the plastic is listed in the same. It is very evident from the figures below that as the particle size decreases the oscillations are also decreased. It is due to the fact that the attached algae is less as compared to bigger sizes. The biofilm thickness is plotted as in section 4.1.1.2.

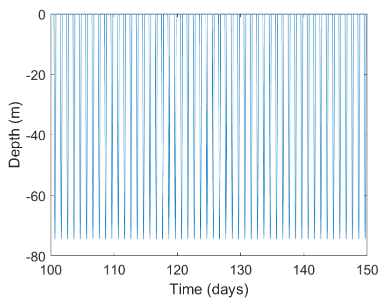

(a)

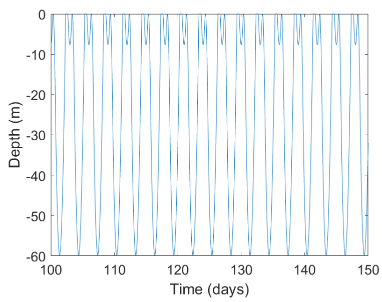

(b)

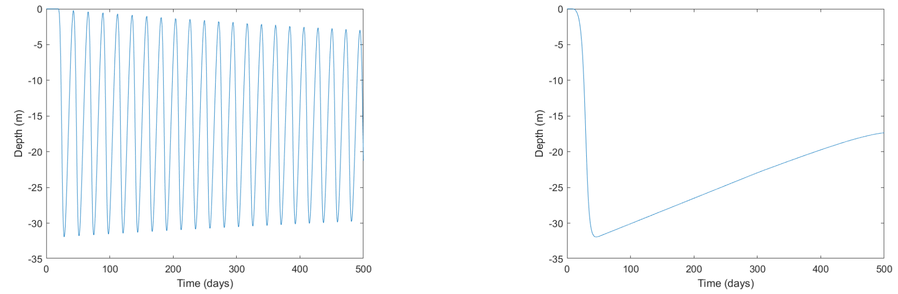

(c) (d)

Figure 4.1: Position of initially buoyant microplastic,PP in Laminar Flow for (a) $r = 1e-3m$ (b) $r = 1e-4m$ (c) $r = 1e-5m$ (d) $r = 1e-6m$

4.1.1.2 Biofilm Thickness

In figure 4.2, the biofilm thickness of PP plastic for different sizes can be seen for a laminar flow case.In accordance with figure 4.1, the oscillations are low due to fact that the thickness of biofilm is less in smaller sizes. It can be seen that the order of magnitude for biofilm thickness of a PP plastic with radius $1e-3m$ is in terms of 10^{-4} while for the same plastic with radius $1e-6m$ is 10^{-6} which clearly explains there is a change in order of magnitude 2.

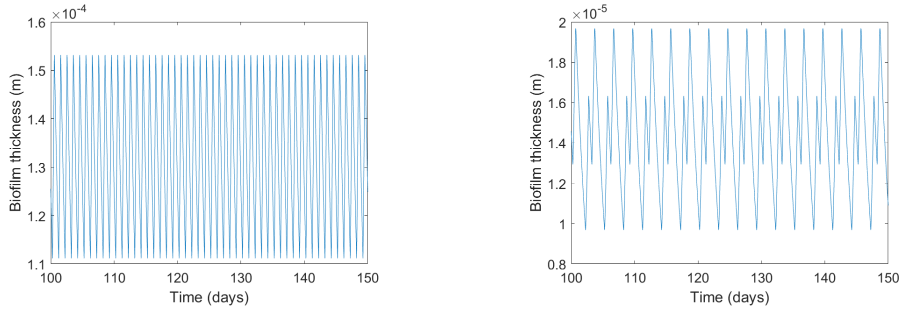

(a) (b)

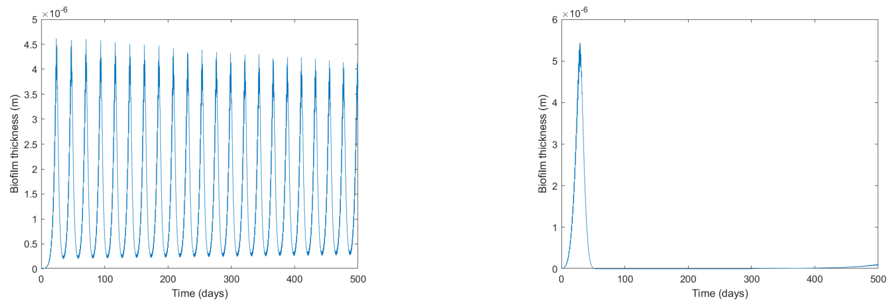

(c) (d)

Figure 4.2: Biofilm Thickness of initially buoyant microplastic,PP in Laminar Flow for (a) $r = 1e-3m$ (b) $r = 1e-4m$ (c) $r = 1e-5m$ (d) $r = 1e-6m$

4.1.1.3 Average Position

The average position is estimated for mainly two reasons. One is that to find the average position of the particle at a particular time since the particle is oscillating. Second reason is that, it helps in determining the convergence of the simulation. The average position of each PP plastic is plotted as in figure 4.3.

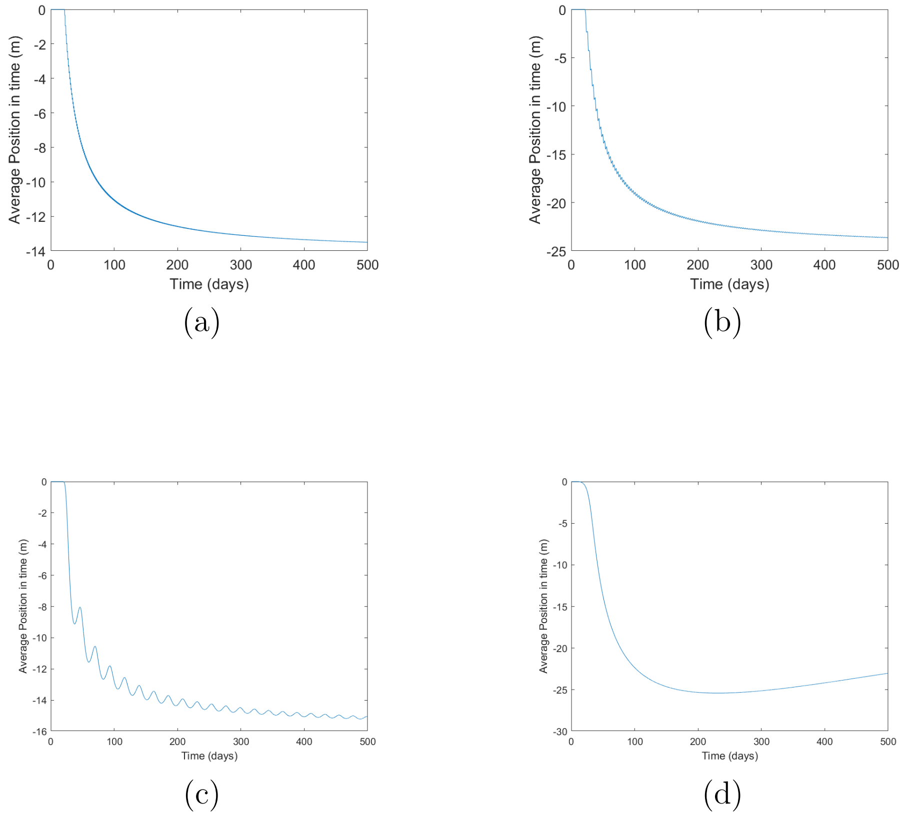

Figure 4.3: Average position of initially buoyant microplastic,PP in Laminar Flow for (a) $r = 1e-3m$ (b) $r = 1e-4m$ (c) $r = 1e-5m$ (d) $r = 1e-6m$

4.1.1.4 Time Fraction

Once the average position of the microplastic if found out, another interesting factor is the time fraction. As been discussed it is the fraction time in which the plastic stays below $z = 0m$ depth (actually $z = 1m$ for better approximation). The time fraction for the initially buoyant microplastic PP is as plotted in figure 4.4.It is inferred that the particle is sinking more when the size of the plastic is reduced. The maximum fraction time achieved by the comparatively biggest particle ($radius = 1e-3m$) is 0.3 while the smallest particle with ($radius = 1e-6m$) has a maximum time fraction close to 0.9 upon convergence.Therefore upon reducing size of the plastic the fraction time is increased which ensures that the particle will sink more if the size is too small.

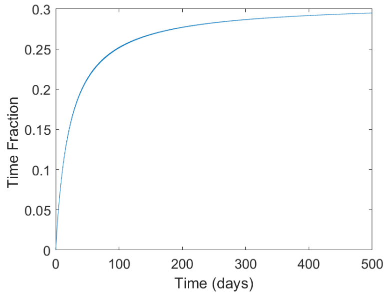

(a)

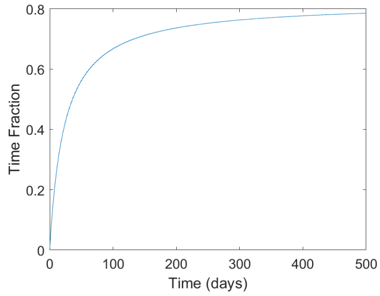

(b)

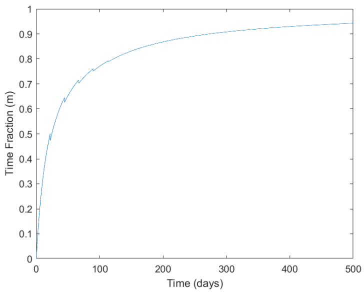

(c)

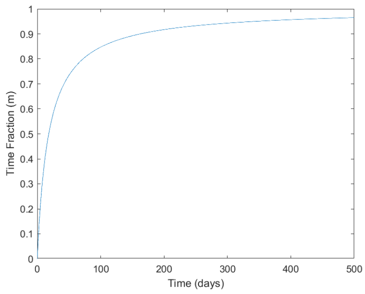

(d)

Figure 4.4: Time Fraction of initially buoyant microplastic,PP in Laminar Flow for (a) $r = 1e - 3m$ (b) $r = 1e - 4m$ (c) $r = 1e - 5m$ (d) $r = 1e - 6m$

4.1.2 LDPE Plastic

LDPE plastic is also initially buoyant. Similar to PP plastic all the statistics are extracted. Only the particle position and time fraction is plotted below in figures 4.5 and 4.6.

4.1.2.1 Plastic Position

LDPE shows similar behaviours as of PP since the particle position or the oscillations are less for smaller sized plastic.

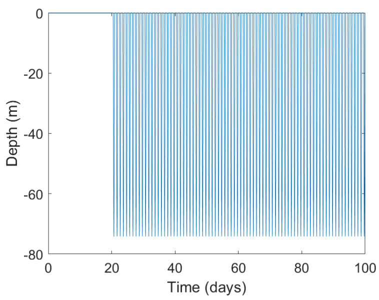

(a)

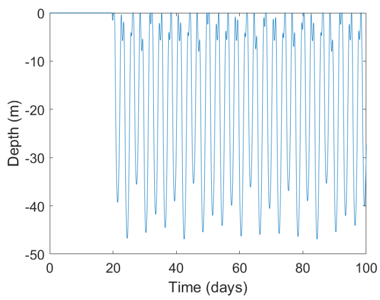

(b)

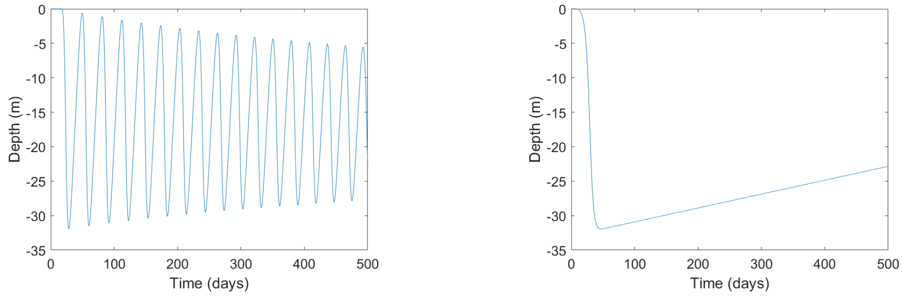

(c) (d)

Figure 4.5: Position of initially buoyant microplastic,LDPE in Laminar Flow for (a) $r = 1e-3m$ (b) $r = 1e-4m$ (c) $r = 1e-5m$ (d) $r = 1e-6m$

4.1.2.2 Time Fraction

The similarity of trend of PP Plastic is repeating here for LDPE also. Comparatively bigger sized one stays less time under $z = 0m$ while the smallest one stays longer time as the maximum value of time fraction ranges from 0.4 to 0.9 approximately while size is decreased.

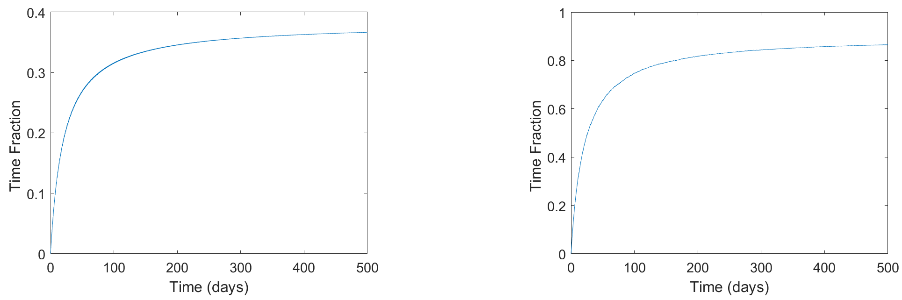

(a) (b)

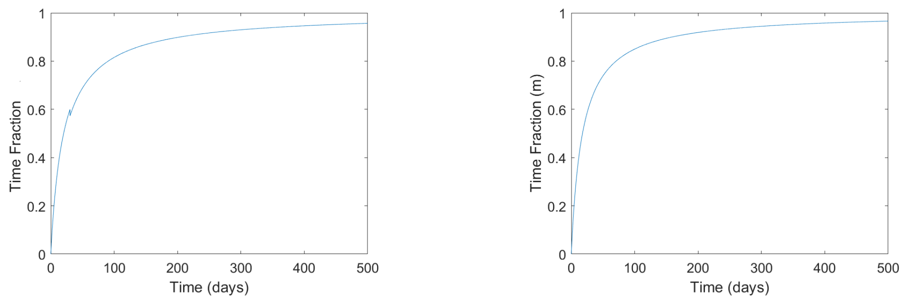

(c) (d)

Figure 4.6: Time Fraction of initially buoyant microplastic,LDPE in Laminar Flow for (a) $r = 1e-3m$ (b) $r = 1e-4m$ (c) $r = 1e-5m$ (d) $r = 1e-6m$

4.1.3 PS Plastic

The non buoyant plastic PS is simulated 500 days similar to the other two cases and the statistics are plotted.

4.1.3.1 Plastic Position

From figure 4.7 it is evident that for PS plastic with radius $1e-3m$, the plastic is sinking right after $t=0$ while on decreasing size it can be seen that there is a very slight delay in sedimentation. It is because of the low sedimentation velocity of the particle.

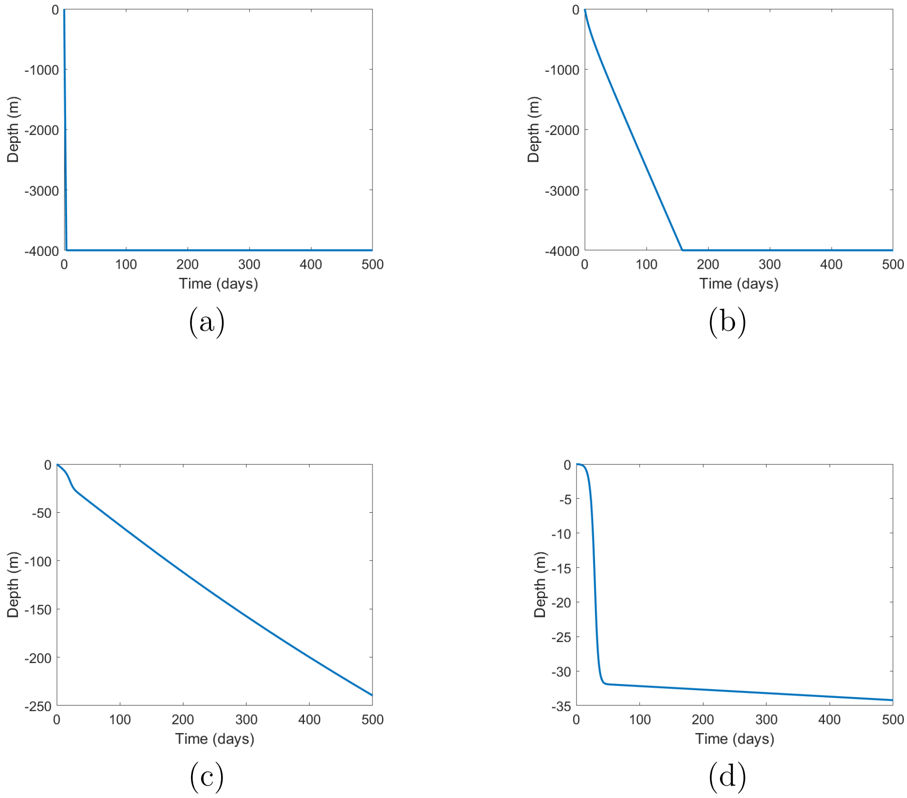

Figure 4.7: Position of non-buoyant microplastic,PS in Laminar Flow for (a) $r = 1e-3m$ (b) $r = 1e-4m$ (c) $r = 1e-5m$ (d) $r = 1e-6m$

4.1.3.2 Time Fraction

The PS plastic with radius $1e-3$ is having a constant time fraction of unity (refer figure 4.8). It states that the plastic is under the water $z=0m$ throughout the computational days. PS $r=1e-4m$ is also having a similar plot, like for almost all days the time fraction is unity while for the smallest particle, since it takes some days to start settling there is delay in reaching maximum fraction time unlike others.

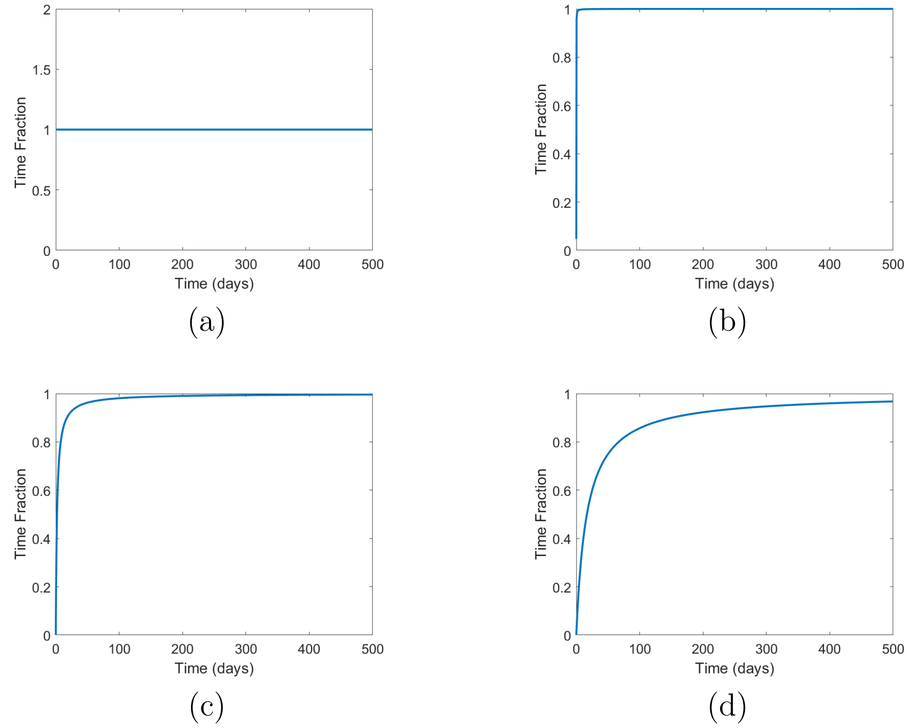

Figure 4.8: Time Fraction of non-buoyant microplastic,PS in Laminar Flow for (a) $r = 1e - 3m$ (b) $r = 1e - 4m$ (c) $r = 1e - 5m$ (d) $r = 1e - 6m$

4.1.4 PVC Plastic

The non buoyant plastic PVC is simulated similar to all other cases. It has been simulated from $t = 0$ to $t = 500$ days. In figure 4.9, the particle trajectory of PVC plastic for different sizes ($r = 1e-3m$ to $r = 1e-6m$) is shown while in figure 4.10, the fraction time for the same is depicted.

4.1.4.1 Plastic Position

In figure 4.9, the particle position of PVC plastic with radius $1e-3m$ to $1e-6m$ is shown. It resembles the other non-buoyant plastic PS. Hence it can be seen that for all non-buoyant plastics, the particle starts to settle soon as the size of the plastic increases.

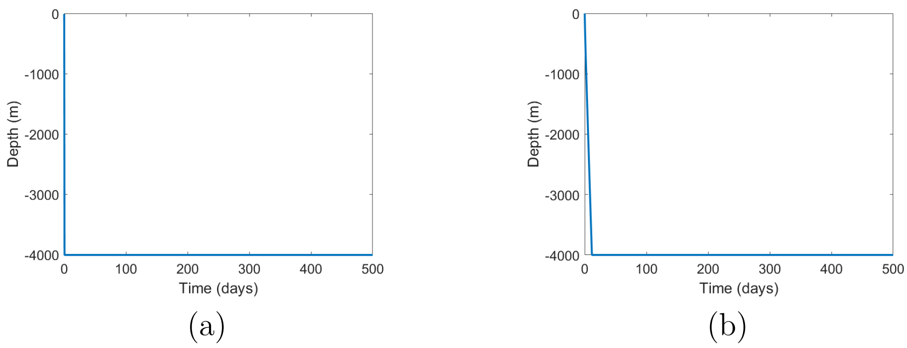

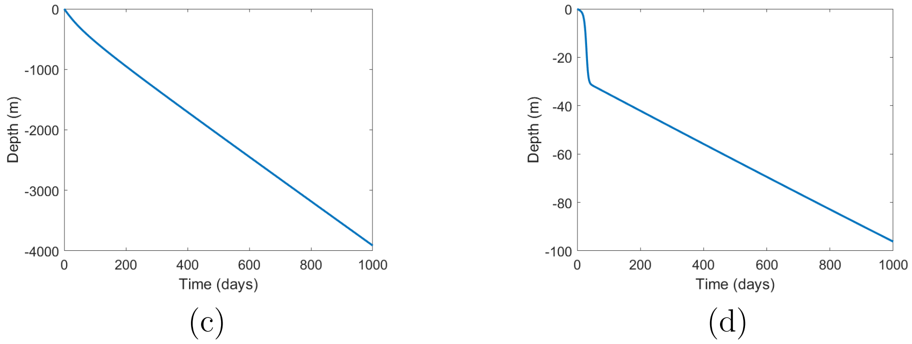

Figure 4.9: Position of non-buoyant microplastic,PVC in Laminar Flow for (a) $r = 1e - 3m$ (b) $r = 1e - 4m$ (c) $r = 1e - 5m$ (d) $r = 1e - 6m$

4.1.4.2 Time Fraction

The PVC plastic with radius $1e-3$ is having a constant time fraction of unity (refer figure 4.10) which is same as the case of PS plastic. PVC $r = 1e - 4m$ is marked bold since fraction time was almost equal to one most of the times and for $t = 1$ the graph was a straight line so close to y-axis. So, in order for better visibility it is marked bold.

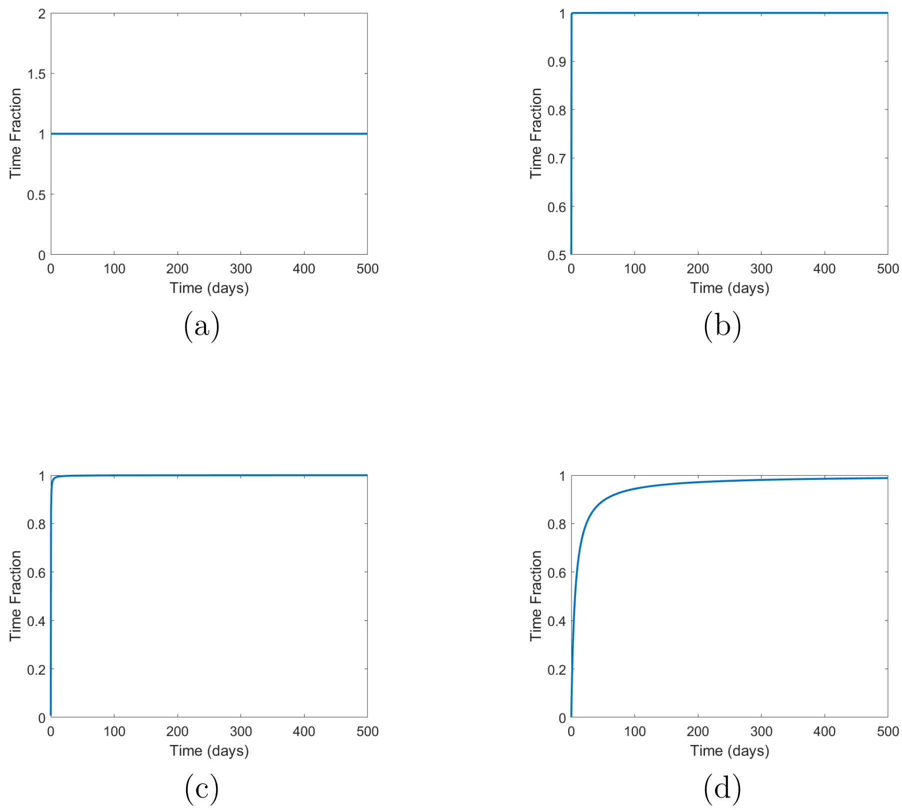

Figure 4.10: Time Fraction of non-buoyant microplastic,PVC in Laminar Flow for (a) $r = 1e - 3m$ (b) $r = 1e - 4m$ (c) $r = 1e - 5m$ (d) $r = 1e - 6m$

4.2 Turbulent Flow Case

As discussed in Section 3.5, the Langevin equation is incorporated into matlab using Monte Carlo simulation and the statistics are extracted. Some of the plots are shown below.

4.2.1 Particle Position

The particle position of PP plastic and PS plastic for the biggest particles ($r = 1e-3, 1e-4m$) are plotted in figure 4.11. Similar to Laminar case, the matching factor is that, more oscillations are occurred.

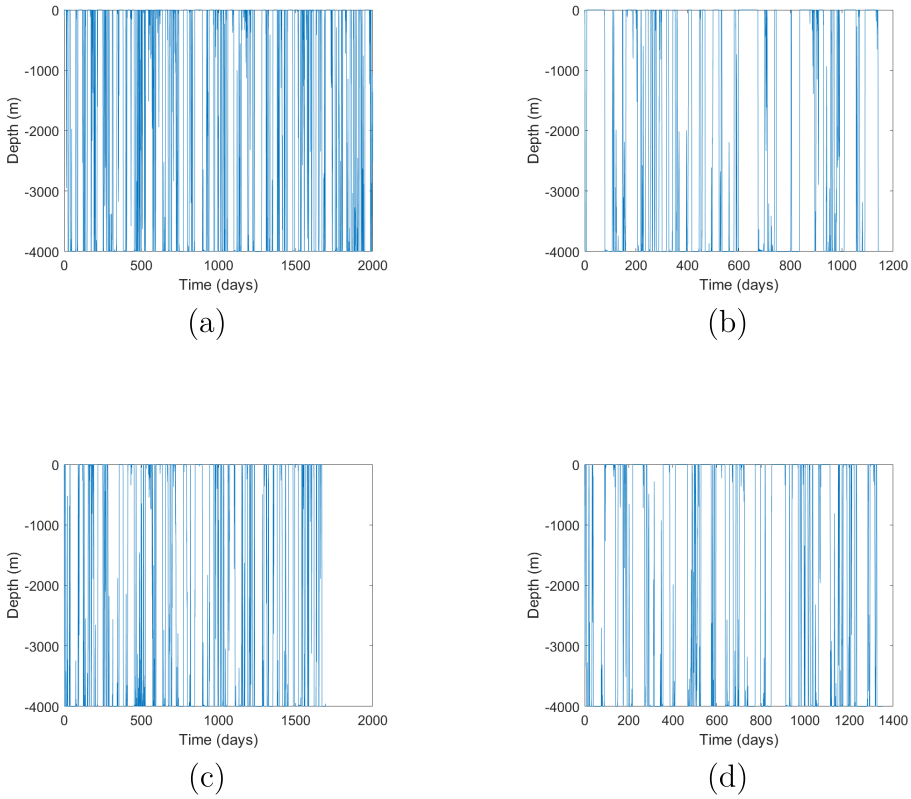

Figure 4.11: Position of microplastics in Turbulent Flow for (a) PP $r = 1e-3m$ (b) PP $r = 1e-4m$ (c) PS $r = 1e-3m$ (d) PS $r = 1e-4m$

4.2.2 Biofilm Thickness

The biofilm thickness for the above plots are also shown here (figure 4.12). It is found out that the attached algae or the biofilm thickness is almost same for all the cases. Hence the turbulent fluctuations have high preference here since the oscillations are different for these two particles.

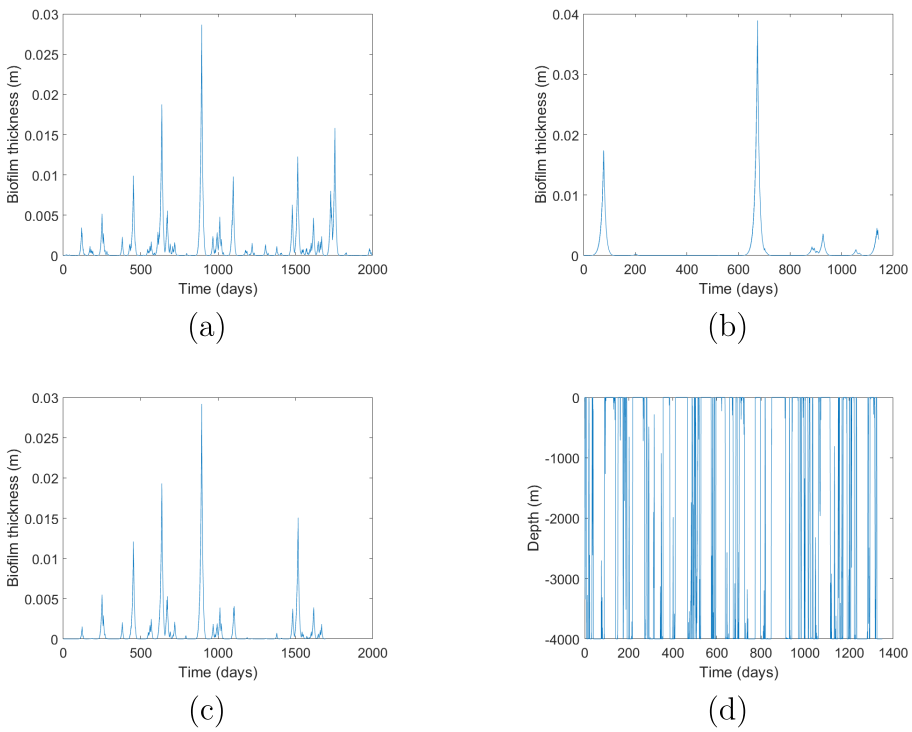

Figure 4.12: Biofilm thickness of microplastics in Turbulent Flow for (a) PP $r = 1e-3m$ (b) PP $r = 1e-4m$ (c) PS $r = 1e-3m$ (d) PS $r = 1e-4m$

4.2.3 Total Density

The total density of both PP and PS plastics are plotted as in figure 4.13. The effect of biofouling is strongly seen in the plastic for turbulent flow cases. It is very evident from the figures that the density of the particle is altering almost every time. This is due to the density of the attached algal mat and its attachment and detachment due to several factors.

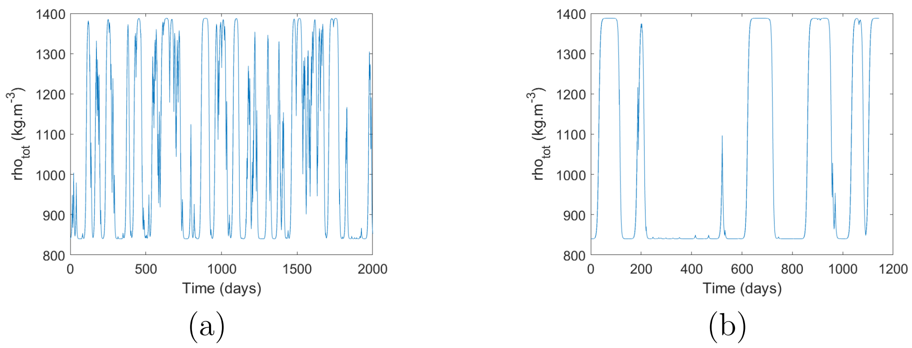

4.2.4 Velocity

The settling velocity of both PP and PS plastics are plotted as in figure 4.14. Unlike the case of quiescent flow, here the larger negative sedimentation velocity when

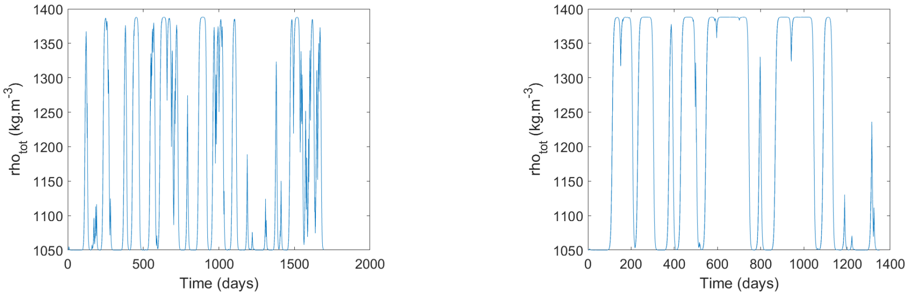

(c) (d)

Figure 4.13: Velocity of microplastics in Turbulent Flow for (a) PP $r = 1e - 3m$ (b) PP $r = 1e - 4m$ (c) PS $r = 1e - 3m$ (d) PS $r = 1e - 4m$

particle reaches its maximum depth to transported back upwards is negligible as compared to the turbulent fluctuations of the flow.

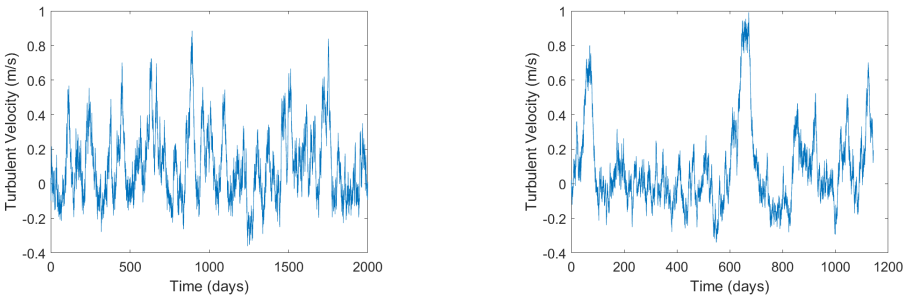

(a) (b)

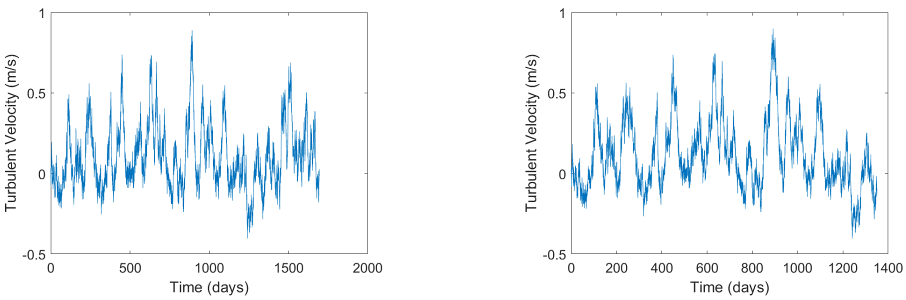

(c) (d)

Figure 4.14: Velocity of microplastics in Turbulent Flow for (a) PP $r = 1e - 3m$ (b) PP $r = 1e - 4m$ (c) PS $r = 1e - 3m$ (d) PS $r = 1e - 4m$

4.2.5 Time Fraction

The results for fraction time is also inline with the other initially buoyant particle PP . Here also on smaller radius, the plot looks same and hence it is confirmed that the initially buoyant particles behave similarly when smaller sizes are simulated.

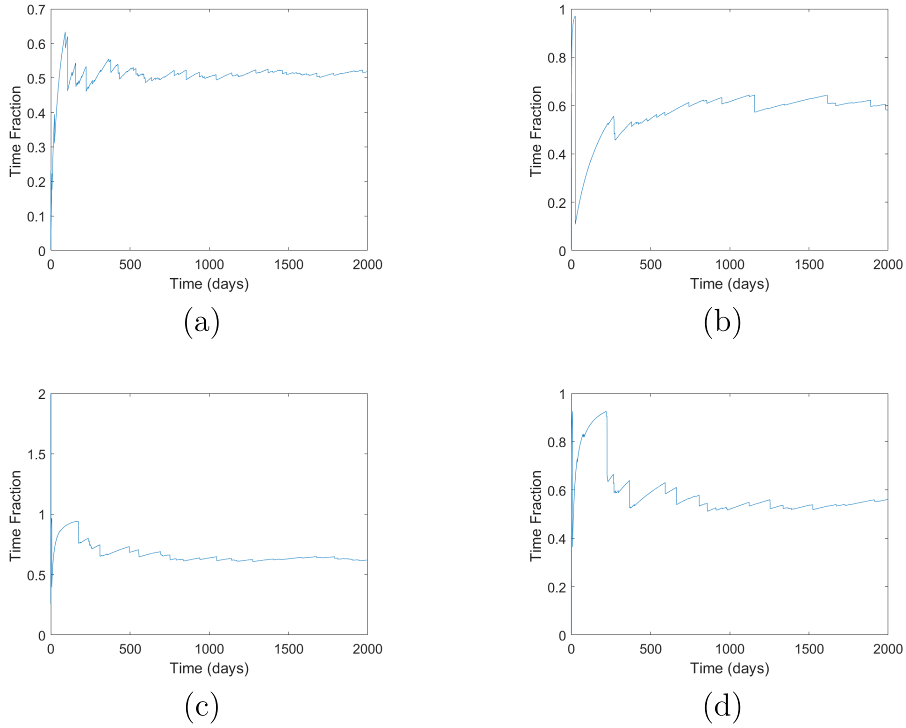

Figure 4.15: Time Fraction of initially buoyant microplastic in Turbulent Flow for (a) PP $r = 1e - 3m$ (b) PP $r = 1e - 4m$ (c) PS $r = 1e - 3m$ (d) PS $r = 1e - 4m$

4.3 Effect of Radius

The effect of biofouling on particle radius when turbulence flow condition is used is found out. It is as shown in figures 4.17 and 4.16 where all the types of plastic shown similar behaviour than the bigger ones.

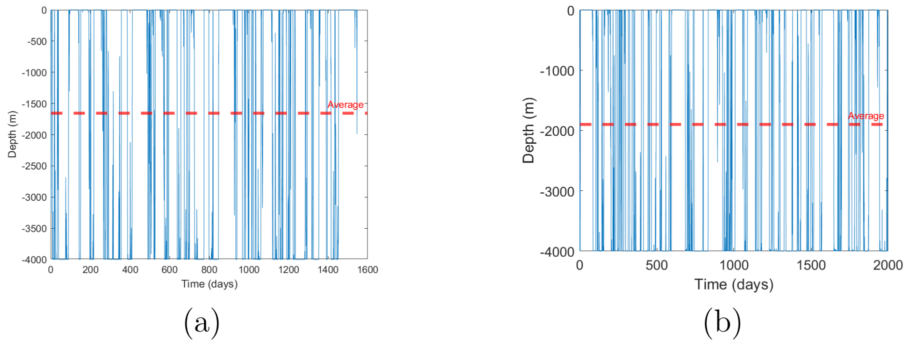

From figures 4.17 and 4.16, it is evident that when $r = 1e - 5, 1e - 6m$, whatever the plastic it maybe (PP,LDPE,PS,PVC) the average position of the microplastic remains approximately same. It substantiates the statement in Results section that when turbulence flow case is considered, the turbulence in the carrier phase is dominated and it doesn't depend on the particle velocity to determine the particle position. Plastics with $r = 1e - 5m$ also showed similar statistics.

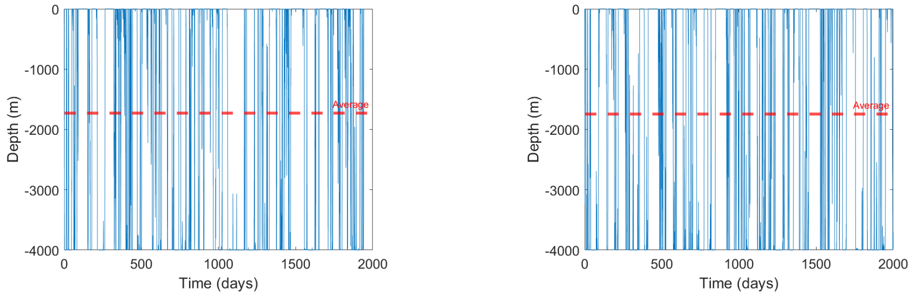

(c) (d)

Figure 4.16: Comparison of particle position in turbulent cases of size $r = 1e-5m$ for (a) PP plastic (b) LDPE plastic (c) PS plastic (d) PVC plastic

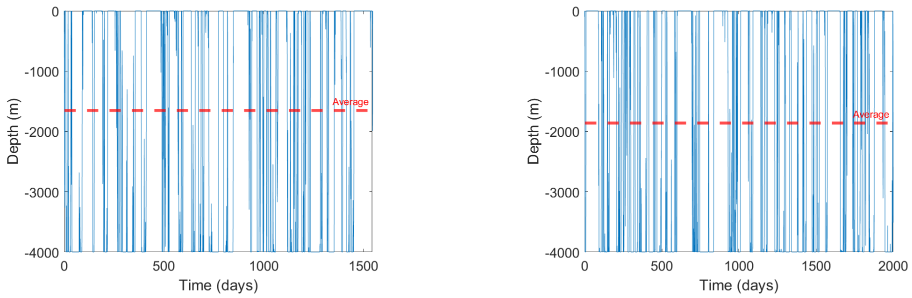

(a) (b)

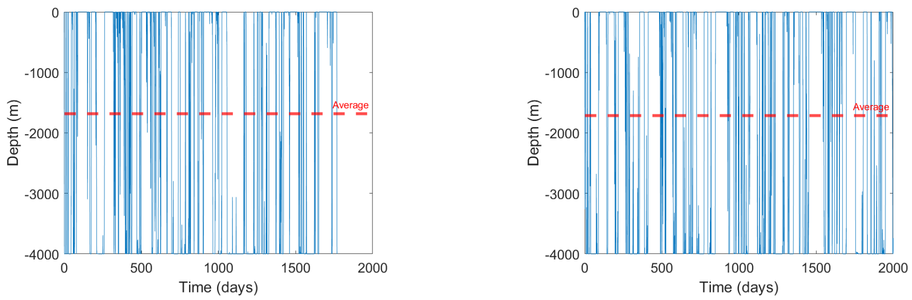

(c) (d)

Figure 4.17: Comparison of particle position in turbulent cases of size $r = 1e-6m$ for (a) PP plastic (b) LDPE plastic (c) PS plastic (d) PVC plastic

The average position is compared with laminar and turbulent cases as depicted in figure 4.18. Most of the cases showed a trend that the particles in laminar flow case is closer to ocean base so that it doesn't travel much deeper into the ocean. But only for plastics with size $r = 1e-3m$ and $r = 1e-4m$ the non-buoyant plastics in the laminar case are at the ocean surface and more close to the ocean surface respectively.

The probability density function of the total radius of the plastics for radius $1e-3m$ is estimated, normalized and plotted as in figure 4.19. The PDF function implies that the plastic is more likely to find in the given frequency range. It is inferred

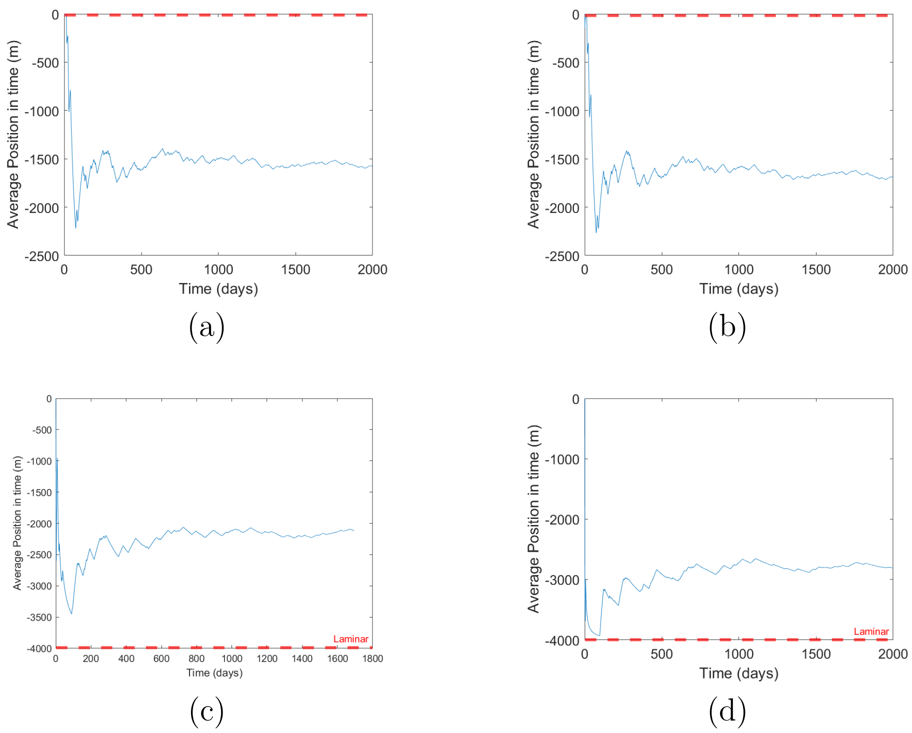

Figure 4.18: Comparison of average position of particle in laminar and turbulent cases of size $r = 1e-3m$ for (a) PP plastic (b) LDPE plastic (c) PS plastic (d) PVC plastic

that the spectrum of the radius in turbulence is much broader than in the laminar case (more than an order of magnitude) with a long exponential tail in the PDF. This implies a larger sedimentation velocity of the particle that scales as radius is increased.

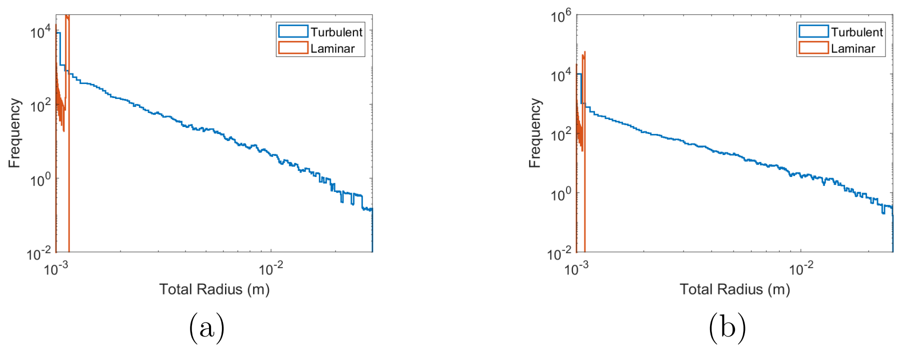

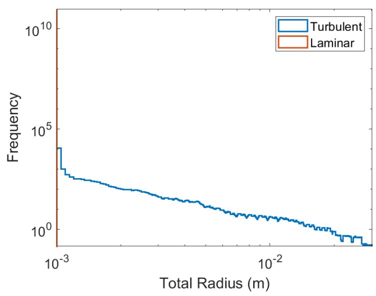

(c)

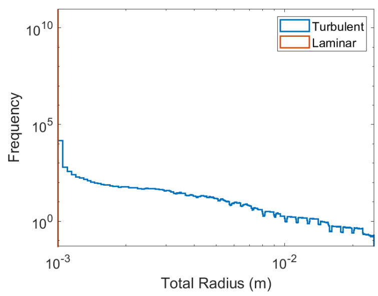

(d)

Figure 4.19: Comparison of probability density function of particle in laminar and turbulent cases of size $r = 1e-3m$ for (a) PP plastic (b) LDPE plastic (c) PS plastic (d) PVC plastic

5

Conclusion

The primary objective of the project is successfully done. Microplastic particles are tracked for various plastics such as initially buoyant PP and LDPE along with non-buoyant PS and PVC. The oscillations of the particles due to alternative biofouling and defouling phenomena is substantiated with the particle position plots discussed in the Results section. The findings can contribute to a sustainable environment by effective removal of the plastics from oceans since the particle trajectory can be estimated.

The study has been done effectively on laminar and turbulent flow conditions with explicit third order low storage Runge-Kutta scheme (which replaced the ode23 in-built solver in matlab because to incorporate the turbulent fluctuation in an easier way) assuming all particles are spherical and thus by determining an equivalent diameter to estimate the sinking velocity. The multiphase study has been done through Lagrangian Particle Tracking Method via one way coupling.

The turbulent flow condition has been modelled with a stochastic approach using Monte Carlo simulation incorporating Langevin equations in Matlab. The turbulent flow simulation results are much more physical in reality. From the obtained results it is clear that when the plastic particle radius is small ($r = 1e - 5m$ and $r = 1e - 6m$), the results looks similar independently on the density ratios. That means for both buoyant and non-buoyant plastics, the results are independent on the type of plastic when the particles smaller in size. Therefore, it is concluded that the turbulent fluctuations are dominant and the sediment velocity of the particle is negligible, thus meaning the particles behaves more as tracers. Thus the preferential zones of accumulation of these microplastics are found out.

The future works from this study includes the usage of drag correction factor due to stratification and the CFD analysis of the same.

Bibliography

[1] Bakelite: *The World's First Synthetic Plastic*. American Chemical Society National Historic Chemical Landmarks.

[2] Andrés Cózar, Fidel Echevarría, J. Ignacio González-Gordillo, Xabier Irigoien, Bárbara Úbeda, Santiago Hernández-León, Álvaro T. Palma, Sandra Navarro, Juan García-de-Lomas, Andrea Ruiz, María L. Fernández-de-Puelles, and Carlos M. Duarte. *Plastic debris in the open ocean.* http://www.pnas.org/lookup/suppl/doi:10

[3] Maynard A *Nanotechnology: a research strategy for addressing risk. Woodrow Wilson International Center for Scholars Project on Emerging Nanotechnologies*

[4] Gregory M *Plastic 'Scrubbers' in Hand Cleansers: a further (and minor) source for marine pollution identified*Mar. Poll. Bull. 32 (12), 867–871.

[5] Merel Kooi et al; *Ups and Downs in the Ocean: Effects of Biofouling on Vertical Transport of Microplastics* DOI: 10.1021/acs.est.6b04702 Environ. Sci. Technol. 2017, 51, 79637971

[6] M. Kooi, E.H. van Nes, M. Scheffer, A.A. Koelmans, 2017. Ups and downs in the ocean: Effects of biofouling on the vertical transport of microplastics, Environmental Science Technology 51 (14), 7963-7971.

[7] A.L. Andrady, 2011. Microplastics in the marine environment, Marine Pollution Bulletin 62 (8), 1596-1605

[8] N. Schmidt, D. Thibault, F. Galgani, A. Paluselli, R. Sempere, 2018. Occurrence of microplastics in surface waters of the Gulf of Lion (NW Mediterranean Sea), Progress in Oceanography, Elsevier, MERMEX special issue, 163, 214-220.

[9] Amy *Microplastic pollution in the Northeast Atlantic Ocean: Validated and opportunistic sampling*Marine Pollution Bulletin 88 (2014) 325–333

[10] Muthukumar *Fouling and stability of polymers and composites in marine environment*Int. Biodeter. Biodegrad. 65 (2), 276–284.

[11] Cotter, Brennan, *"Ethical Problems with Plastic in the Ocean"* (2019)Senior Theses. 113 doi.org/10.33015/dominican.edu/2019. HCS.ST.06

[12] BOURDREL Florian. *Study on vertical oscillations and horizontal trajectories of passive virtual particles in the Gulf of Naples: investigation of biofouling effect and Lagrangian dispersion.* Stazione Zoologica Napoli Anton Dohrn (SZN)

[13] Stephan Juricke, Sergey Danilov, Anton Kutsenko, Marcel Oliver *Ocean kinetic energy backscatter parametrizations on unstructured grids:Impact on mesoscale turbulence in a channel*Ocean Modelling 138 (2019) 51–67

[14] Maren Walter and Christian Mertens *Mid-depth mixing linked to North Atlantic Current variability* GEOPHYSICAL RESEARCH LETTERS, VOL. 40, 4869–4875, doi:10.1002/grl.50936, 2013

[15] R.A. Shaw, Annu. Rev. Fluid Mech. 35. 183(2003)

[16] Gaetano Sardina, Francesco Picano, Luca Brandt and Rodrigo Caballero *Continuous Growth of Droplet Size Variance due to Condensation in Turbulent Clouds* American Physical Society 2015,DOI: 10.1103/PhysRevLett.115.184501

[17] Hojun Lee, Itzhak Fouxon and Changhoon Lee *Sedimentation of a small sphere in stratified fluid*American Physical Society. DOI:10.1103/PhysRevFluids.4.104101

[18] R. Mehaddi1, F. Candelier and B. Mehlig *Inertial drag on a sphere settling in a stratifed fuid*J. Fluid Mech. (2018), vol. 855, pp. 10741087.

[19] Young Kyoung Song, Sang Hee HONG, Soeun Eo, Mi Jang, Gi Myung Han, Atsuhiko Isobe, and Won Joon Shim. *Horizontal and vertical distribution of microplastics in Korean coastal waters* Characterization of Natural and Affected Environments DOI: 10.1021/acs.est.8b04032

[20] Kiørboe, T.; Tang, K.; Grossart, H. P.; Ploug, H.*Dynamics of microbial communities on marine snow aggregates: Colonization, growth, detachment, and grazing mortality of attached bacteria.*Appl. Environ. Microbiol. 2003, 69 (6), 30363047.

[21] James, S. C.; Boriah, V.*Modeling algae growth in an open channel raceway*J. Comput. Biol. 2010, 17 (7), 895906.

[22] Bechet, Q.; Shilton, A.; Guieysse, B*Modeling the effects of light and temperature on algae growth:*.State of the art and critical assessment for productivity prediction during outdoor cultivation. Biotechnol. Adv. 2013, 31 (8), 16481663.

[23] Dietrich, W. E.*Settling velocity of natural particles.*Water Resour. Res. 1982, 18 (6), 16151626.

[24] Kowalski, N.; Reichardt, A. M.; Waniek, J. J.*Sinking rates of microplastics and potential implications of their alteration by physical, biological, and chemical factors.*Mar. Pollut. Bull. 2016, 109 (1), 310319.

[25] Uitz, J.; Claustre, H.; Morel, A.; Hooker, S. B. *Vertical distribution of phytoplankton communities in open ocean:*An assessment based on surface chlorophyll. J. Geophys. Res. 2006, 111,C8.

[26] Ardyna, M.; Babin, M.; Gosselin, M.; Devred, E.; Belanger, S.; Matsuoka, A.; Tremblay, J.-E.*Parameterization of vertical chlorophyll a in the Arctic Ocean:impact of the subsurface chlorophyll maximum on regional, seasonal, and annual primary production estimates* Biogeosciences 2013, 10 (6), 4383.

[27] Bernard, O.; Remond, B *Validation of a simple model accounting for light and temperature effect on microalgal growth*Bioresour. Technol. 2012, 123, 520527.

[28] Thompson, R. C.; Olsen, Y.; Mitchell, R. P.; Davis, A.; Rowland, S. J.; John, A. W. G.; McGonigle, D.; Russell, A. E. *Lost at sea: where is all the plastic?* Science 2004, 304 (5672), 838.

A
Appendix 1

A.1 Constant values for Temperature, Salinity and Density

For the North Pacific, the following parameters are used

A.1.1 Temperature

The constant values or the parameters of temperature profile are as given in table A.1

Parameters	**Value**
p	2
z_c	-300
T_{surf}	25
T_{bot}	1.5

Table A.1: Parameter values of Temperature Profile

A.1.2 Salinity

The constant values or the parameters of Salinity profile are as given in table A.2

Parameters	**Value**
z_{fix}	-1000
S_{fix}	34.6
$c1$	9.9979979767e-17
$c2$	1.0536246487e-12
$c3$	3.9968286066e-09
$c4$	6.5411526250e-06
$c5$	4.1954014008e-03
$c6$	3.5172984035e+01

Table A.2: Parameter values of Salinity Profile

A.1.3 Density

The constant values or the parameters of Density profile are as given in table A.3

Parameters	**Value**
$a1$	9.999e+02
$a2$	2.034e-02
$a3$	-6.162e-03
$a4$	2.261e-05
$a5$	-4.657e-08
$b1$	8.020e+02
$b2$	-2.001
$b3$	1.677e-02
$b4$	2.261e-05
$b5$	-4.657e-05

Table A.3: Parameter values of Density Profile

B

MATLAB CODES

B.1 Non-Linear Stokes Drag

```
%% NON LINEAR STOKES DRAG
%
        x = abs(rho_tot-density)/density*9.81*(4/9)*((r_pl*r0)^3)/((nu0*viscosity_kin)^2);
% Finding Reynolds Number
    func = @(Rep) real(1*Rep^1 + 0.15*Rep^1.687 - x);
    x0 =1;
    roots = fzero(func,x0);
    w_sink= nu0*viscosity_kin*roots/(2*r_pl*r0);
    if (rho_tot<density)
            w_sink=-w_sink;
    end
            w_sink=-w_sink*t0/z0; %dimensionless velocity
```

B.2 MAIN CODES

The main codes are listed below in subsections with function names where the two files are common for both laminar and turbulent cases and the one one which is different is listed separately.

B.2.1 Result File

```
clear all;
clc;


r_pl=1e-3;
%
%
% for biofouling ode, we can try different days of insemination: 0 (1st
% january), 90 (1st April), 181 (1st july), 273 (1st october)


time=zeros(1,length(r_pl));
t_initial=[0 90 181 273];
k=1; %to choose the initial day of insemination



%% PP
%          for i=1:length(r_pl)
%           [time(i),~]=biofouling_ode_ad_2_modified(0,2000,r_pl(i),840,1,23);
% end

%% LDPE
% for i=1:length(r_pl)
%          [time(i),~]=biofouling_ode_ad_2_modified(0,1000,r_pl(i),920,1,23);
% end

%% PS
% for i=1:length(r_pl)
%          [time(i),~]=biofouling_ode_ad_2_modified(0,2000,r_pl(i),1050,1,23);
% end

%% PVC
for i=1:length(r_pl)
        [time(i),~]=biofouling_ode_ad_2_modified(0,2000,r_pl(i),1380,1,23);
end
```

B.2.2 f_ode_ad_2_modified

```
function [g,t_bf,rho_tot] = f_ode_ad(ff,r_pl,rho_pl,i,t)

        r0=r_pl; %characteristic scale of all quantities related to plastic size
        rho0=1000; %characteristic scale of all densities (water and plastic)
        z0=10; %characteristic scale of depth
        t0=1*24*3600; %characteristic scale of time
        mu0=1e-3; %characteristic scale of dynamic viscosity
        nu0=1e-6; %characteristic scale of kinematic viscosity
        T0=20+273; %characteristic scale of kelvin temperature
        na_amb0=1e-7; %characteristic scale of the inverse of ambient algae concentration

        r_pl=r_pl/r0; %dimensioneless plastic radius
        rho_pl=rho_pl/rho0; %dimensionless plastic density


% *** Parameters ***
% All units are the ones used in the article of Kooi et al (2017)

        kappa = 1.38064852e-23;       % Boltzman constant

% Light

        light_Im = 1.2e+8;            % Surface light intensity at noon
        ext_water = 0.2;              % Extinction coefficient water

% Algae growth

        mu_max = 1.85;                % Maximum growth rate
        alpha = 0.12;                 % Initial slope in growth equation
        mort_alg = 0.39;              % Mortality rate
        resp_alg = 0.1;               % Respiration rate
        Q_10 = 2;                     % Temperature coefficient respiration
        temp_min = 0.2;               % Minimum temperature algae growth
        temp_opt = 26.7;              % Optimal temperature algae growth
        temp_max = 33.3;              % Maximum temperature algae growth
```

```
        light_Iopt = 1.75392e+13;     % Optimal light intensity algae growth

% Algae properties

        C_cell = 2726e-9;             % mg carbon for a single cell
        vol_alg = 2.0e-16/r0^3;       % dimensionless volume individual algae
        rho_bf = 1388.0/rho0;         % dimensionless biofilm density

        shear = 1.7e+5;               % shear used in encounter rate

% Converts from day^-1 to second^-1

        sec_per_day = 86400.0;
        light_Im=light_Im/sec_per_day;
        mu_max=mu_max/sec_per_day;
        alpha=alpha/sec_per_day;
        mort_alg=mort_alg/sec_per_day;
        resp_alg=resp_alg/sec_per_day;
        light_Iopt=light_Iopt/sec_per_day;
        shear=shear/sec_per_day;

% Rending dimensionless these quantities:
        light_Im=light_Im*t0;
        mu_max=mu_max*t0;
        alpha=alpha*t0;
        mort_alg=mort_alg*t0;
        resp_alg=resp_alg*t0;
        light_Iopt=light_Iopt*t0;
        shear=shear*t0;




        %x is the vector of the vectorial differential equation x'=f(x)
        %nalg=x(1);
        %z=x(2);
        nalg=ff(1);
        z=ff(2);

        if(nalg<0) %nalg<0 is not physicall
```

```
            nalg=0;
        end

        if z>0 %plastic can not be higher than sea surface
            z=0;
        end

% Get temperature, salinity and chla
%In this function, climatologies from Kooi et al. are used

            temp=biofouling_temperature(z*z0,i); %z*z0 because these function do not take dimensionless depth
            salt=biofouling_salt(z*z0,i);
            chla=biofouling_chlorophyll(z*z0,i);


% Evaluate density and viscosity from equation of state of seawater
% *** ATTENTION *** convert salinity from g/kg (PSU) to kg/kg

            salt=salt*1.0e-3;
            a1=9.999e+2;
            a2=2.034e-2;
            a3=-6.162e-3;
            a4=2.261e-5;
            a5=-4.657e-8;
            b1=8.020e+2;
            b2=-2.001;
            b3=1.677e-2;
            b4=2.261e-5;
            b5=-4.657e-5;

            density=a1+a2*temp+a3*(temp^2)+a4*(temp^3)+a5*(temp^4)+b1*salt+b2*salt*temp+b3*salt*(temp^2)+b4*salt*(temp^3)+b5*(salt^2)*(temp^2);
            density=density/rho0; %dimensionless sea water density

            viscosity=0.156*(temp+64.993)^2;
            viscosity=4.2844e-5+1.0/(viscosity-91.296);

            a1=1.541+1.998e-2*temp-9.52e-5*(temp^2);
            b1=7.974-7.561e-2*temp+4.724e-4*(temp^2);

            viscosity_dyn=viscosity*(1.0+a1*salt+b1*(salt^2))/
```

```
                mu0; %dimensionless dynamic viscosity



% Light intensity at the surface
             hour=mod((t*t0)/3600,24);
             light_I0=light_Im*sin((hour-6.0)*2.0*pi/24.0); %12 hours day : 6h-18h
%               light_I0=light_Im*sin((hour-4)*pi/16.0); %16 hours day : 4h-20h
%               light_I0=light_Im*sin((hour-8)*pi/8.0); %8 hours day : 8h-16h


            if(light_I0 <0)
               light_I0 = 0;
            end


% Light intensity at the float depth (depth negative)
% *** ATTENTION *** algae induced extinction depending only on local value

             light_Iz=light_I0*exp(ext_water*z*z0);

% Growth rate under optimal temperature conditions

             mu_opt=mu_max*light_Iz/(light_Iz+t0*(mu_max/alpha)*(light_Iz/light_Iopt-1.0)^2);

% Temperature influence on growth rate

             temp_inf=((temp-temp_max)*(temp-temp_min)^2)/((temp_opt-temp_min)*((temp_opt-temp_min)*(temp-temp_opt)-(temp_opt-temp_max)*(temp_opt+temp_min-2.0*temp)));

% Algae growth rate

             mu_tot=mu_opt*temp_inf;

% Conversion factor from chlorophyll to carbon
% *** ATTENTION *** we are supposing that there is NO LIMITATION
% to the growth rate due to NUTRIENTS

```

```
            chla_C=0.003+0.0154*exp(0.05*temp)*exp(-0.059*light_Iz/t0*1.0e-6*sec_per_day)*mu_tot/mu_max;
% Ambient algae concentration (number/m**3)
            na_amb=na_amb0*(chla/chla_C)/C_cell; % dimensionless algae concentration
            if light_Im*exp(ext_water*z*z0)<=0.01*light_Im
                na_amb=0;
            end
% Evaluate the total radius of the particle
            teta_pl=4.0*pi*(r_pl^2);
            v_pl=pi*(r_pl^3)*4.0/3.0;
            v_bf=vol_alg*nalg*teta_pl;
            v_tot=v_bf+v_pl;
            t_bf=nthroot(v_tot*3.0/(4.0*pi),3)-r_pl;
            if(t_bf<0.0)
                t_bf = 0.0;
            end
            r_tot=nthroot(v_tot*3.0/(4.0*pi),3);
            r_alg=(vol_alg*3.0/(4.0*pi))^(1.0/3.0);
            rho_tot=(v_pl*rho_pl+v_bf*rho_bf)/v_tot;
% Equivalent spherical diameter of particle
            viscosity_kin=viscosity_dyn/density;  % dimensionless kinematic viscosity
            d_ast=(rho_tot-density)*9.81*r0^3/nu0^2*(2.0*r_tot)^3;
            d_ast=abs(d_ast/(density*viscosity_kin^2));
% Sinking velocity
```

```
            if (d_ast<5.0e-2)
              om_ast=(d_ast^2)/5832;
            else
              log_d=log10(d_ast);
              om_ast=10^(-3.76715+1.92944*log_d-0.09815*(log_d^2)-0.00575*(log_d^3)+0.00056*(log_d^4));
            end

            w_sink=9.81*nu0*om_ast*viscosity_kin*(rho_tot-density)/density;
            w_sink=-nthroot(w_sink,3)*t0/z0; %dimensionless velocity


% Encounter kernel

            if z*z0>=0 && w_sink>0 %plastic cannot fly
               w_sink=0;
            end

            if z*z0<=-4000 && w_sink<0 %ocean floor set at -4000m as in the biofouling paper
               w_sink=0;
            end

            dz=w_sink;



            temp=(temp+273.16)/T0; %dimensionless kelvin temperature
            beta_alg_brownian=2/3*(temp/viscosity_dyn)*(1/r_tot+1/r_alg)*(r_tot+r_alg); %dimensionless beta_alg_brownian
            beta_alg_settling=0.5*pi*r_tot^2*abs(w_sink); %dimensionless beta_alg_settling
            beta_alg_shear=4/3*shear*(r_tot+r_alg)^3; %dimensionless beta_shear


% New value of right-hand side of algae growth equation

            collision=(beta_alg_brownian*(kappa*T0*t0)/mu0+beta_alg_settling*z0*r0^2+beta_alg_shear*r0^3)*na_amb/(na_amb0*teta_pl); %dimensionless collision term
```

```
        growth=mu_tot*nalg; %dimensionless growth term
        mortality=mort_alg*nalg; %dimensionless mortality term
        respiration=resp_alg*nalg*Q_10^((temp*T0-20-273.16)*0.1); %dimensionless respiration term


        dnalg=collision+growth-mortality-respiration; %dimensionless dA/dt



        g=[dnalg;dz]; %new value for x'=f(x)


end
```

B.3 Laminar case

B.3.1 biofouling_ode_ad_2_modified

```
function [t_init,w_sink_max]=biofouling_ode_ad_2_modified_RK3(zinit,tlim,r_pl,rho_pl,i,ode)

%in this program we use climato from Kooi et al (value of i, for my report I chose i=1 for North Pacific climato)
%equations are dimensionless: it allows ode to solve smallest radii
%(r_pl=1e-6 for instance)

t_init=0.;
w_sink_max=0.;
tlim=tlim*24*3600; %conversion from days to seconds

t0=1*24*3600; %characteristic time scale
z0=10; %characteristic space scale
rho0=1000; %characteristic scale of all densities (water and plastic)

tlim=tlim/t0; %dimensionless limit time


%Coefficients
ark(1)=8/15;
```

```
ark(2)=5/12;
ark(3)=3/4;
brk(1)=0;
brk(2)=-17/60;
brk(3)=-5/12;


f0=[0;zinit/z0]; %initial conditions: nalg0=0 and z0=zinit

ff=f0;   %LHS Initializing
g=[0;0]; %RHS Initializing
Re=zeros(1,length(r_pl));%Re
rho_tot=zeros(1,length(r_pl));
t_bf=zeros(1,length(r_pl));

tspan=[0 tlim]'; %interval of integration

avg_pos = 0;
sumT1=0;
deltat=0.001; %deltat
itout=10; %printing interval
tt=0;
itmax=round(tlim/deltat);
    %for it=1:itmax.....
     for k=1:itmax
    zi=ff(2)*z0;
       for rki=1:3

          pf = ff+brk(rki)*g*deltat;
    % We need for the RHS g(t) f_ode_ad_2(t,x,r_pl,rho_pl,i);...
     ...I guess you need to put g in the function call;
          [g,t_bf,rho_tot]= f_ode_ad_2_modified(ff,r_pl,rho_pl,i,tt);

          ff = pf+ark(rki)*g*deltat;

            if ff(2)>0.  %plastic cannot fly
                ff(2)=0.;
                g(2)=0;
            end

       end
          zf=ff(2)*z0;

         avg_pos = avg_pos + (ff(2)*z0);
```

```
        avg_pos_time = avg_pos/k;

         if zi<-1 && zf<-1
             sumT1=sumT1+deltat;
             T1=sumT1/tt;
             dlmwrite('Frac_time.csv',T1,'-append');
         end

     tt=tt+deltat;
    % t, position, velocity to be printed in a text file
         if(mod(i,itout)==1)

       dlmwrite('t.csv',tt,'-append');
       dlmwrite('velocity.csv',g(2)*z0/t0,'-append');
       dlmwrite('position.csv',ff(2)*z0,'-append');
       dlmwrite('nalg.csv',ff(1)/r_pl^2,'-append');
       dlmwrite('tbf.csv',t_bf*r_pl,'-append');          % Biofilm Thickness saved as csv
       dlmwrite('rhop.csv',rho_tot*rho0,'-append');  %Total plastic density saved as csv
       dlmwrite('avg_pos_time.csv',avg_pos_time,'-append'); %Average Position saved as csv


         end




     end


    %% Files concatenated together

     dlmwrite('PVC_1e-5.csv', [csvread('t.csv'),csvread('velocity.csv'),csvread('position.csv'),csvread('nalg.csv'),csvread('tbf.csv'),csvread('rhop.csv'),csvread('avg_pos_time.csv')],'Delimiter',' ');

         delete('t.csv');
         delete('velocity.csv');
         delete('position.csv');
         delete('nalg.csv');
         delete('tbf.csv');
         delete('rhop.csv');
         delete('avg_pos_time.csv');
```

```
A=dlmread('PP_1e-6.csv'); %Read the new scv file
col1 = A(:, 1);   %Time
col2 = A(:, 2);   %Velocity
col3 = A(:, 3);   %Position
col4 = A(:, 4);   %Nalg
col5 = A(:, 5);   %T_Bf
col6 = A(:, 6);   %Rho_p
col7 = A(:, 7);   %Avg_pos_time


 B=dlmread('Frac_time.csv'); %Read the new csv file
 col8 = B(:, 1);   %Fraction Time

%% Plots

%Plot of Velocity
figure(1)
Velocity=plot(col1,col2)
hold on;
%xlim([20,25])
ylabel('Velocity (m.s^{-1})')
xlabel('Time (days)')
saveas(Velocity,'Velocity_1e-5_RungeKutta_PVC.png');

%Plot of Depth
figure(2)
Depth=plot(col1,col3)
hold on;
ylabel('Depth (m)')
xlabel('Time (days)')
saveas(Depth,'Settling_1e-5_RungeKutta_PVC.png');

%Plot of nalg
figure(3)
Algae=plot(col1,col4)
hold on;
%xlim([20,25])
ylabel('Number of attached algae by surface unit (m
    ^{-2})')
xlabel('Time (days)')
saveas(Algae,'No_Attached_Algae_1e-5_Rungekutta_PVC.png
    ');

```

```
%Plot of t_bf
figure(4)
Tbf=plot(col1,col5)
hold on;
ylabel('Biofilm thickness (m)')
xlabel('Time (days)')
saveas(Tbf,'Biofilm_Thickness_1e-5_Rungekutta_PVC.png')
    ;

%Plot of rho_tot
figure(5)
Rho_Total=plot(col1,col6)
hold on;
%xlim([20,25])
%ylim([970,1030])
ylabel('rho_{tot} (kg.m^{-3})')
xlabel('Time (days)')
saveas(Rho_Total,'Plastic_Total_Density_1e-5
    _Rungekutta_PVC.png');

%Plot of Avg_Pos
figure(6)
Avgpos=plot(col1,col7)
hold on;
ylabel('Average Position in time (m)')
xlabel('Time (days)')
saveas(Avgpos,'Average_Position_1e-5_Rungekutta_PVC.png
    ');

%Plot of Time_Frac
figure(7)
time = linspace(0,tlim,length(col8));
T_Frac=plot(time,col8)
hold on;
ylabel('Time Fraction (m)')
xlabel('Time (days)')
saveas(T_Frac,'Time_Fraction_1e-6_Rungekutta_PP.png');

figure(8)
Pdf_rho=histogram(col6, 'normalization', 'pdf');
ylabel('Frequency')
xlabel('Density (kg.m^{-3})')
saveas(Pdf_rho,'PDF_rho_1e-5_Rungekutta_PVC.png');

figure(9)
col5=col5+(r_pl);
```

```
        Pdf_Rtotal=histogram(col5, 'normalization', 'pdf');
        ylabel('Frequency')
        xlabel('Total Radius (m)')
        saveas(Pdf_Rtotal,'PDF_rtotal_1e-5_Rungekutta_PVC.png');


       %
%         Frac_T=sprintf('Fraction Time at end=%d',T1);
%         disp(Frac_T);

end
```

B.4 Turbulent case

The same biofouling function is given as,

```
function [t_init,w_sink_max]=biofouling_ode_ad_2_modified(zinit,tlim,r_pl,rho_pl,i,ode)

%in this program we use climato from Kooi et al (value of i, for my report I chose i=1 for North Pacific climato)
%equations are dimensionless: it allows ode to solve smallest radii
%(r_pl=1e-4 for instance)

t_init=0.;
w_sink_max=0.;
tlim=tlim*24*3600; %conversion from days to seconds

t0=1*24*3600; %characteristic time scale
z0=10; %characteristic space scale
rho0=1000; %characteristic scale of all densities (water and plastic)

tlim=tlim/t0; %dimensionless limit time


% RK3 Coefficients
ark(1)=8/15;
ark(2)=5/12;
ark(3)=3/4;
brk(1)=0;
brk(2)=-17/60;
brk(3)=-5/12;

```

```
f0=[0;zinit/z0]; %initial conditions: nalg0=0 and z0=zinit

ff=f0;   %LHS Initializing
g=[0;0]; %RHS Initializing
Re=zeros(1,length(r_pl));%Re
rho_tot=zeros(1,length(r_pl));
t_bf=zeros(1,length(r_pl));

tspan=[0 tlim]'; %interval of integration

%Turbulent part
vturb=0;
pvturb=0;
gturb=0;
avg_pos = 0;
sumT1=0;

deltat=0.001; %deltat
itout=10; %printing interval
tt=0;
itmax=round(tlim/deltat);
     %for it=1:itmax.....
     for k=1:itmax

       for rki=1:3
%Turbulent velocity
           zi=ff(2)*z0;
           pvturb=vturb+brk(rki)*gturb*deltat;
           if rki==1
                 stoc=normrnd(0.,1.);
           end

           [T0,vrms]=rhs_turb(ff,i);


           gturb=-vturb/T0+vrms*sqrt(2./(T0*deltat))*stoc;




           pf = ff+brk(rki)*g*deltat;


           [g,t_bf,rho_tot]= f_ode_ad_2_modified(ff,r_pl,rho_pl
              ,i,tt);
```

```

        g(2)=g(2)+vturb;

        ff = pf+ark(rki)*g*deltat;
        vturb=pvturb+ark(rki)*gturb*deltat;

          if ff(2)*z0>0.  %plastic cannot fly
              ff(2)=0.;
              %g(2)=0;
          end
          if ff(2)*z0<-4000.  %plastic cannot sink further
              ff(2)=-4000./z0;
              %g(2)=0;
          end


      end
       zf=ff(2)*z0;

       avg_pos = avg_pos + (ff(2)*z0);
       avg_pos_time = avg_pos/k;

        if zi<-1 && zf<-1
            sumT1=sumT1+deltat;
            T1=sumT1/tt;
            dlmwrite('Frac_time.csv',T1,'-append');
        end
    tt=tt+deltat;

   % t, position, velocity to be printed in a text file
        if(mod(i,itout)==1)

      dlmwrite('t.csv',tt,'-append')
      dlmwrite('velocity.csv',(g(2)-vturb)*z0/t0,'-append')
      dlmwrite('position.csv',ff(2)*z0,'-append')
      dlmwrite('nalg.csv',ff(1)/r_pl^2,'-append')
      dlmwrite('tbf.csv',t_bf*r_pl,'-append')         %
         Biofilm Thickness saved as csv
      dlmwrite('rhop.csv',rho_tot*rho0,'-append')  %Total
         plastic density saved as csv
      dlmwrite('vturb.csv',vturb*z0/t0,'-append')
      dlmwrite('avg_pos_time.csv',avg_pos_time,'-append');
         %Average Position saved as csv

        end
    end
```

```
    %% Files concatenated together

    dlmwrite('PVC_1e-4_turb.csv', [csvread('t.csv'),csvread(
       'velocity.csv'),csvread('position.csv'),csvread('nalg
       .csv'),csvread('tbf.csv'),csvread('rhop.csv'),csvread
       ('vturb.csv'),csvread('avg_pos_time.csv')],'Delimiter
       ',',');

        delete('t.csv');
        delete('velocity.csv');
        delete('position.csv')
        delete('nalg.csv')
        delete('tbf.csv')
        delete('rhop.csv')
        delete('vturb.csv')
        delete('avg_pos_time.csv')

    A=dlmread('PVC_1e-4_turb.csv');  %Read the new csv file
    col1 = A(:, 1);   %Time
    col2 = A(:, 2);   %Velocity
    col3 = A(:, 3);   %Position
    col4 = A(:, 4);   %Nalg
    col5 = A(:, 5);   %T_Bf
    col6 = A(:, 6);   %Rho_p
    col7 = A(:, 7);   %v_turb
    col8 = A(:, 8);   %avg_pos

    B=dlmread('Frac_time.csv');  %Read the new csv file
    col9 = B(:, 1);   %Fraction Time

    %% Plots

    %Plot of Velocity
    figure(1)
    Velocity=plot(col1,col2)
    hold on;
%     xlim([20,25])
    ylabel('Velocity (m.s^{-1})')
    xlabel('Time (days)')
    saveas(Velocity,'Velocity_1e-4_RungeKutta_PVC_turb.png'
       );

    %Plot of Depth
    figure(2)
    Depth=plot(col1,col3)
    hold on;
```

```
    % yline(-1600,'-.r','Average','LineWidth',2);
    ylabel('Depth (m)')
    xlabel('Time (days)')
    saveas(Depth,'Settling_1e-4_RungeKutta_PVC_turb.png');

    %Plot of nalg
    figure(3)
    Algae=plot(col1,col4)
    hold on;
%     xlim([20,25])
    ylabel('Number of attached algae by surface unit (m^{-2})')
    xlabel('Time (days)')
    saveas(Algae,'No_Attached_Algae_1e-4_Rungekutta_PVC_turb.png');

    %Plot of t_bf
    figure(4)
    Tbf=plot(col1,col5)
    hold on;
    ylabel('Biofilm thickness (m)')
    xlabel('Time (days)')
    saveas(Tbf,'Biofilm_Thickness_1e-4_Rungekutta_PVC_turb.png');

    %Plot of rho_tot
    figure(5)
    Rho_Total=plot(col1,col6)
    hold on;
%     xlim([20,25])
%     ylim([970,1030])
    ylabel('rho_{tot} (kg.m^{-3})')
    xlabel('Time (days)')
    saveas(Rho_Total,'Plastic_Total_Density_1e-4_Rungekutta_PVC_turb.png');

    %Plot of v_turb
    figure(6)
    v_turb=plot(col1,col7)
    hold on;
    ylabel('Turbulent Velocity (m/s)')
    xlabel('Time (days)')
    saveas(v_turb,'Turbulent_Velocity_1e-4_Rungekutta_PVC_turb.png');

    %Plot of Avg_Pos
```

```
        figure(7)
        Avgpos=plot(col1,col8)
        hold on;
        %yline(-14,'-.r','Laminar','LineWidth',2);
        ylabel('Average Position in time (m)')
        xlabel('Time (days)')
        saveas(Avgpos,'Average_Position_1e-4_Rungekutta_PVC_turb.png');

        %Plot of Time_Frac
        figure(8)
        time = linspace(0,tlim,length(col9));
        T_Frac=plot(time,col9);
        hold on;
        %yline(0.29503,'-.r','Laminar','LineWidth',2);
        ylabel('Time Fraction (m)')
        xlabel('Time (days)')
        saveas(T_Frac,'Time_Fraction_1e-4_Rungekutta_PVC_turb.png');

        figure(9)
        col5=col5+(r_pl);
        Pdf_Rtotal=histogram(col5, 'normalization', 'pdf');
        ylabel('Frequency')
        xlabel('Total Radius (m)')
        saveas(Pdf_Rtotal,'PDF_rtotal_1e-4_Rungekutta_PVC.png');

        figure(10)
        Pdf_rho=histogram(col6, 'normalization', 'pdf');
        ylabel('Frequency')
        xlabel('Density (kg.m^{-3})')
        saveas(Pdf_rho,'PDF_rho_1e-4_Rungekutta_PVC.png');
end
```

B.4.1 rhs_turb

```
function [T0,vrms] = rhs_turb(ff,i)

          z0=10; %characteristic scale of depth
          tt0=1*24*3600; %characteristic scale of time

          z=ff(2);

          %kin=0.01; %Turbulent kinetic energy in m2/s2 this should be function of z*z0....
```

```
kin=kin_turb(ff,i);



        %eps=1.E-7; %Turbulent dissipation rate in m2/s3 or W/Kg
eps=eps_turb(ff,i);
        %Viscosity calculation
          temp=biofouling_temperature(z*z0,i); %z*z0 because these function do not take dimensionless depth
          salt=biofouling_salt(z*z0,i);

          salt=salt*1.0e-3;
          a1=9.999e+2;
          a2=2.034e-2;
          a3=-6.162e-3;
          a4=2.261e-5;
          a5=-4.657e-8;
          b1=8.020e+2;
          b2=-2.001;
          b3=1.677e-2;
          b4=2.261e-5;
          b5=-4.657e-5;

          density=a1+a2*temp+a3*(temp^2)+a4*(temp^3)+a5*(temp^4)+b1*salt+b2*salt*temp+b3*salt*(temp^2)+b4*salt*(temp^3)+b5*(salt^2)*(temp^2);

          viscosity=0.156*(temp+64.993)^2;
          viscosity=4.2844e-5+1.0/(viscosity-91.296);

          a1=1.541+1.998e-2*temp-9.52e-5*(temp^2);
          b1=7.974-7.561e-2*temp+4.724e-4*(temp^2);

          viscosity_dyn=viscosity*(1.0+a1*salt+b1*(salt^2)); %dynamic viscosity
          viscosity_kin=viscosity_dyn/density; %Kinematic viscosity


          Re_lambda=sqrt(20.*kin*kin/(3.*viscosity_kin*eps));
          C0=6.5/(1.+140.*Re_lambda^(-4./3.))^(3./4.);
          T0=4*kin/(3*C0*eps); %in s
          vrms=sqrt(2*kin/3); %in m/s

```

```
            T0=T0/tt0; %nondimensional
            vrms=vrms*tt0/z0; %nondimensional


end
```

B.4.2 kin_turb

```
function kin=kin_turb(ff,i)
        z0=10; %characteristic scale of depth
    z=ff(2);

        if(z*z0==0)
            kin=0.24;
        else if(z*z0>=-200)
               kin=(0.0002.*z*z0) + 0.18;
              else if(z*z0>=-1200 && z*z0<=-200)
                kin=(0.0001.*z*z0) + 0.14;
                 else if (z*z0<=-1200)
                     kin=0.02;
                     end
                end
            end

    end
```

B.4.3 eps_turb

```
function eps=eps_turb(ff,i)


        z0=10; %characteristic scale of depth
    z=ff(2);




    if(z*z0>-800)
            eps=6.6e-9;
        else if(z*z0>=-950 && z*z0<=-800)
                eps=5e-9;
                 else if(z*z0>=-1120 && z*z0<=-950)
                eps=4.3e-9;
                else if(z*z0>=-1285 && z*z0<=-1120)
                eps=3.3e-9;
                 else if(z*z0>=-1600 && z*z0<=-1285)
                eps=3.06e-9;
                 else if(z*z0>=-1740 && z*z0<=-1600)
```

```
                eps=3.46e-9;
                 else if(z*z0>=-2070 && z*z0<=-1740)
                eps=3.85e-9;
                 else if(z*z0>=-2390 && z*z0<=-2070)
                eps=3e-9;
                 else if(z*z0>=-2550 && z*z0<=-2390)
                eps=3.57e-9;
                else if(z*z0>=-3030 && z*z0<=-2550)
                eps=4e-9;
                else if(z*z0>=-3340 && z*z0<=-3030)
                eps=4.15e-9;
                else if(z*z0>=-4000 && z*z0<=-3340)
                eps=3.77e-9;

                    end
                    end
                    end
                     end
                     end
                     end
                     end
                     end
                    end

            end
        end
    end




end
```

DEPARTMENT OF SOME SUBJECT OR TECHNOLOGY
CHALMERS UNIVERSITY OF TECHNOLOGY
Gothenburg, Sweden
www.chalmers.se

CHALMERS
UNIVERSITY OF TECHNOLOGY